A Mathematical Model of Chronic Myelogenous Leukemia

Brent Neiman
University College
Oxford University

Candidate for Master of Science in Mathematical Modelling and Scientific Computing

MSc Dissertation
Supervisor: Dr. Andrew C. Fowler

September, 2000

A mathematician is a machine for turning coffee into theorems

Paul Erdos

Acknowledgements

First, I would like to thank Sir John and Lady Thouron for having founded the Thouron Award as well as their son and grandson, Tiger and Rupert, for continuing their family's commitment to the Award. Without the generosity of the Thouron family I would not have had the opportunity to study at Oxford and to progress my interest and studies in applied mathematics.

As an undergraduate at the Wharton School, I first took an interest in mathematical modelling after learning from and working with Dr. Paul Kleindorfer, a decision scientist. Dr. Kleindorfer spent quite a long time working with me on my applications and helped me tremendously throughout the process.

While I was researching which U.K. program to attend, OCIAM's mathematical modelling program interested me the most, in part because of the world-wide-web page of Andrew Fowler. Though I found the weekly homework assignments for his lecture painfully difficult (argghh), his supervision of my research was clear, energetic, and fun. I am very lucky to have had Dr. Fowler as my supervisor and he is responsible for my having enjoyed this introduction to research and academia.

Finally, I want to thank my parents for all their whole-hearted support. Without their help, I could not have traveled as extensively as I did, spent time learning an instrument, or participated in any of the numerous extra-curricular endeavors which have made this year so rich. Mom and Dad, thank you.

Abstract

Chronic Myelogenous Leukemia (CML) is one of the most common types of leukemia. It is characterized by a chronic, seeemingly stable steady state, which gives rise to oscillatory instability in the hematapoietic stem cell count. There are also many cases of CML which involve oscillations about a steady state during the chronic period (called Periodic Chronic Myelogenous Leukemia). Though instabilities are found frequently in many biological systems, it is rather unusual for the stem cell count in a patient with leukemia to be nonmonotonic over time. As such, the instability in CML is of tremendous interest to mathematical biologists. A more clear understanding of the dynamics of this disease might not only help with the development of treatments or a cure to CML, but it might also be a useful aid in determining what causes instability in other oscillatory diseases such as Cyclical Neutropenia. This paper's aim is to create a mathematical model of CML which might aid us in understanding the mechanism by which the chronic phase of the disease becomes unstable and reaches the acute phase.

Contents

List of Figures

List of Tables

Chapter 1

Introduction

1.1 What is Leukemia?

Each year, approximately 20% of all deaths in prosperous countries around the world are caused by some form of cancer [1]. Most people are aware that cancer cells differ from normal cells in that they are able to reproduce and proliferate without facing the constraints that dictate the growth rate of normal cells. In addition, they invade and develop in parts of the body normally inhabited by other types of cells. Different types of cancers are categorized by the cell types from which they emerge. Cancers arising from hematopoietic cells, the precursors to the various types of blood cells, are called leukemias.

Leukemia is a progressive, malignant disease characterized by a rapid and uncontrolled proliferation and growth of abnormal blood cells. This proliferation occurs in the bone marrow, as well as in the peripheral blood, blood forming organs, and blood filtering organs. The classification of different forms of leukemia relies on the progression of the disease (acute or chronic) as well as the type of cell affected (myeloid, lymphoid, or monocyte).

1.2 Introduction to Chronic Myelogenous Leukemia

Chronic Myelogenous Leukemia (CML), also known as chronic granulocytic leukemia, chronic myeloid leukemia, and chronic myelocytic leukemia, is a disease of the hematopoietic stem cells [36]. Stem cells are characterized by three properties: they are not themselves finished with the process of differentiation; they reproduce and proliferate without limit; and after dividing, each daughter cell can either remain a stem cell or proceed to a terminal differentiation state [1]. Different types of stem cells differentiate to form different types of cells throughout the body. Hematopoietic stem cells are responsible for the formation of the different types of blood cells in the body such as leukocytes (white blood cells), erythrocytes (red blood cells), B-lymphocytes, platelets, and dendritic cells. The leukocytes, which include the T lymphocytes and dendrites, form part of the immune response and serve to prevent infections. They travel in the blood stream, but also can pass into tissues surrounding the circulatory system. There are significantly more erythrocytes than leukocytes and these cells are responsible for carrying oxygen throughout the body. These tiny cells are able to do this because they carry the oxygen-binding protein hemoglobin. Platelets are also very tiny cells and help regulate blood clotting and healing.

The stem cell population is able to replenish itself through a proliferative, self-renewal process (discussed later in detail). CML is characterized by a mutation in the normal hematopoietic stem cell population, which creates a single "abnormal" stem cell. With several exceptions, this abnormal stem cell functions similarly to the original stem cells. One major difference is that it possesses a growth advantage. This competitive advantage leads to a malignant proliferation and subsequently, to the relative dominance of the abnormal stem cell population. Another difference is that the abnormal stem cell population gives rise to some cells that do not differentiate properly. As a result, there is a wide range of clinical results that can lead to the patient's death. Frequently, the abnormal cells do not differentiate at a sufficiently high rate to form healthy levels of white and red blood cells. This results in anemia and in a weakened immune system, vulnerable to infection [8]. Other cases, however, involve the release of immature white blood cells into the peripheral blood and diminished platelet counts. In addition to these conditions, which leave the patient prone to infection and incapable of healing at normal rates, bone pain and tenderness in rhythm with the palpations of the heart can occur due to the expansion of the bone marrow.

Many cases are diagnosed as a result of routine blood tests during the early, asymptomatic, portion of the disease [11]. Diagnosis involves testing the dividing cells in the bone marrow for the Philadelphia (Ph) chromosome, the hallmark of CML. Humans possess 46 chromosomes in the cell nucleus, each containing a molecule of DNA that transmits genetic information. The Ph chromosome is a reciprocal translocation that relocates the ABL gene from chromosome 9 to chromosome 22, adjacent to the BCR gene. This means that the ABL proto-oncogene, which is found on the 9th chromosome, abnormally fuses with the interrupted end of the BCR (breakpoint cluster region) of chromosome 22 [1]. This fusion results in new BCR-ABL transcript codes that create a chimeric protein. This protein has a tyrosine kinase activity (which indirectly affects a cell's decision to live or die, or to proliferate or stay quiescent [1]) that is significantly greater than the normal protein has and seems to have the property of an oncogene growth factor. Generally, molecular probing of the BCR gene can detect alterations, which can lead to a positive diagnosis of CML. CML is an acquired disease as identical twins and offspring of Ph-positive patients do not carry the chromosome.

The disease typically progresses through three phases: the chronic phase, the acceleration phase, and the acute phase. Figure 1.1 shows the progression in time through these three phases. Periodic Chronic Myelogenous Leukemia (pCML) differs slightly in that the chronic phase involves periodic oscillations with a period of about three months [9]. The chronic phase of pCML also concludes with a very rapid progression to an acute phase. *Here we must emphasize that this progression is not very well defined and is only vaguely representable in a graph. As such, figure 1.1 should not mislead the reader into thinking that the disease develops according to any well-defined pattern. Rather, the important characteristics of the graphic are the existence of a slow-progressing chronic phase, the following instability, and transition to the acute phase.*

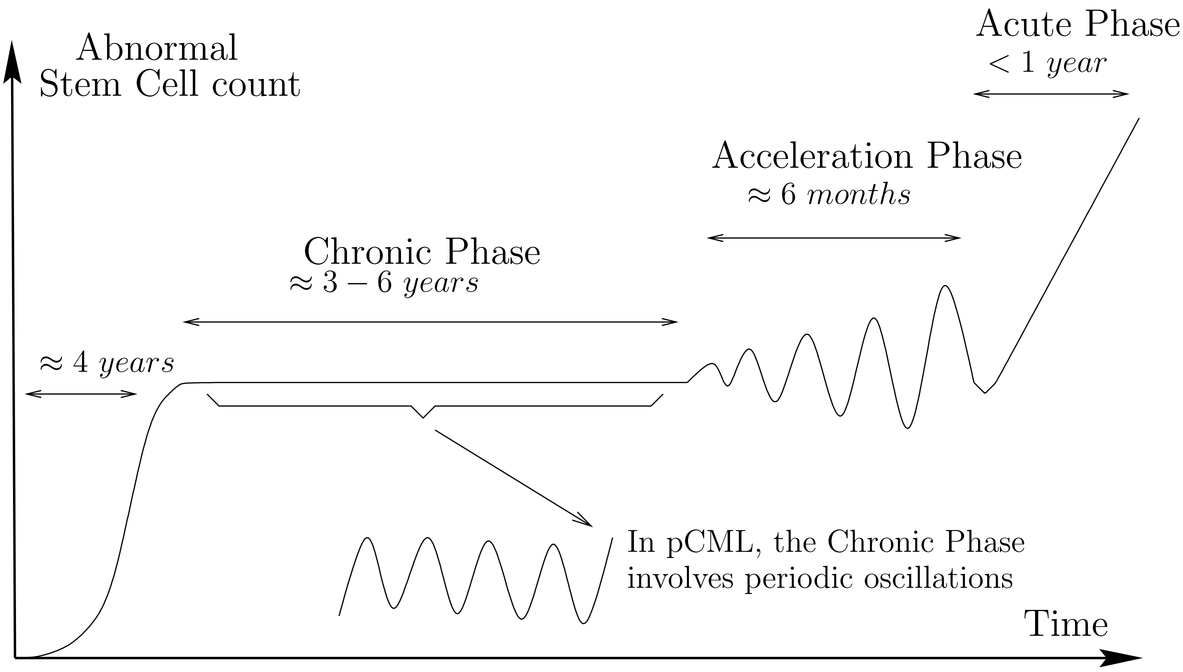

Figure 1.1: CML progresses through three distinct phases. After a relatively quick rise in the cell count, the system reaches a seemingly steady state. After several years, however, this steady state, called the chronic phase, gives rise to oscillatory instability. Ultimately, this leads to the acute phase which is a sharp, usually fatal, increase in the cell count.

1.2.1 The Chronic Phase

After the initial stem cell mutation occurs, the abnormal cells proliferate and become increasingly dominant. This proliferation is accompanied by a steady rise in the amount of leukocytes and platelets, as well as an increase in the white cell count. This period of growth, lasting approximately four years, is frequently referred to as the preclinical period and generally transpires before a diagnosis of CML is made. Ultimately, however, the amount of abnormal stem cells, already dominant, seems to level off and reach a steady state. Alternatively, in pCML, the dominant stem cells oscillate periodically throughout the chronic phase. Untreated, the disease exhibits this apparent stability for three to six years [6].

1.2.2 The Acceleration Phase

At some point, the stability of the chronic phase gives way to instability known as the accelerated phase. The count of abnormal stem cells may suddenly rise or fall, and then continues to oscillate unpredictably for about six months [12].

1.2.3 The Acute Phase

The acceleration gives way to an acute phase when the abnormal stem cell count explodes upward. During this phase, the cells usually exhibit further mutations and usually have a "differentiation blocked" phenotype which significantly reduces the differentiation rate of the stem cells (discussed later in more detail). The acute phase often lasts from three to six months and generally leads to the patient's death.

Our interest in the modelling of CML is to formulate a plausible explanation of the transition from the seemingly stable chronic phase to the unstable acceleration phase and ultimately, to the rapidly changing acute phase. We know that the abnormal cells grow at the expense of the normal cells. At some point, where the abnormal cells outnumber the normal cells, there appears to be stability for a period of time before the state becomes unstable. From a mathematical modelling perspective, this immediately causes us to search for a slow moving variable. Our hope is that we can find a quasi-equilibrium which moves through the parameter space with the drift of the slow variable. If this quasi-equilibrium folds over itself, there is the chance that the slow drift of a variable could cause the system to "fall off" the equilibrium leading to instability or rapid growth.

Chapter 2

Possible Causes of the Instability?

Initially, we have many ideas as to what might be the key slowly moving variable that leads to instability. One idea is that the time delay needed for a cell to reproduce could be altered by the same mutation that causes the growth advantage in CML [4]. Hence, there is the possibility that a continuously changing time delay for replication in the abnormal stem cells could cause oscillatory instability. Indeed, time delays frequently lead to instabilities in biological and ecological processes. The immune response is also an obvious place to look for this slowly moving variable. When we include the immune system into our model, it will involve significantly more dimensions than our initial models. As such, it seems plausible to reach a pseudo-equilibrium state, where one of the many variables continues to slowly vary. Other less promising yet reasonable places to look for this variable include the slow exhaustion of the stem cell niche (a physical space which stem cells occupy when receiving growth factors), as well as the idea of a continuous, though very low, mutation rate. This low mutation rate could slowly lead to further mutations which limit differentiation or allow abnormal cells to produce their own growth factors.

2.1 Time Delay

Like many self-regulating biological systems, the rate of reproduction in hematopoietic stem cells is controlled by a negative feedback loop. This means that at any given time, the population of stem cells is evaluated and if this population is greater than a certain threshold, future production will be reduced. Conversely, if the population lies below the threshold, more cells will begin the process of self-renewal. This mechanism serves to maintain the stem cell population at some optimal level while smoothing out both positive and negative perturbations from this level. The process of self-replication, though, takes a non-trivial amount of time. Hence, when new cells are entering the system, they are entering based on slightly outdated information. As such, certain values for the delay most likely exist which would give rise to an instability in this system.

2.2 The Immune Response

The myeloid progenitor and the common lymphoid progenitor are two types of hematopoietic stem cells in the bone marrow. These cells are the precursors of a number of lymphocytes including B lymphocytes and T lymphocytes. Each T lymphocyte expresses a single antigen receptor close to its outer surface, specific to a particular antigen. Initially during the T cell population's formation, a vast range of potential antigen recognition receptors is formed. As the developmental process proceeds, though, if a lymphocyte's receptor binds with an antigen that is already part of the healthy biological system, or a self-antigen, it is removed [22]. This helps to ensure that all the lymphocytes are "self-tolerant" and will only attack what is genuinely "foreign" to the body. After the process is complete, the T cell population as a whole has receptors that can recognize a great number of antigens. This broad and diverse range is called "the T cell repertoire." This type of T cell elimination or inactivation also occurs after development and may underlie the apparent tolerance that the immune system sometimes develops to tumor cells such as CML. In this case, tolerance may be a gradual process developing during the course of the disease.

Similarly, the hematopoietic stem cells give rise to entities called interdigitating reticular cells, or dendrites. Dendrites possess a degree of "self-knowledge" due to a similar developmental mechanism as is present in T cell formation. Dendrites move around in the marrow and in peripheral blood and consume dead entities. When one of these entities, a virus, for example, is recognized as foreign, the dendrites express proteins which indicate to the T cells what has been found. When one of the T cells "sees" the abnormal protein on the dendrites, which corresponds to its particular receptor, it is "activated." This activation involves cellular progression to become a lymphoblast, which then proliferates through mitosis. As it carries the receptor for the detected antigen, all its progeny carry the same receptor. This increased population of antigen-specific cells gives rise through differentiation to effector cells, which actually kill the antigen. Upon elimination of the antigen, the population wanes back to a normal state. In CML, increasing amounts of antigen-presenting cells will be derived from the malignant clone and therefore, the immune system's self-knowledge will reflect the characteristics of the abnormal cells. Thus, as the disease progresses, the abnormal dendritic cells will dominate, and the amount of cells that recognize CML to be abnormal will be significantly decreased or eliminated. In this manner, the specific immune response to CML will be progressively eroded.

2.3 The Exhausting of the Stem Cell Niche

Stem cells receive essential growth and differentiation factors from a stem cell niche. For the purposes of our model, we may simply think of these niches as a limited resource, such as food. In the absence of CML, all cells are able to access these niches. However with such prolific amounts of total stem cells in the CML case (both normal and abnormal), some threshold may be reached where cells are not able to receive their growth and differentiation factors properly.

2.4 Production of New Growth Factors

Primitive cells from CML might be able to synthesize their own growth factors. As the number of abnormal cells increases, the total growth factor concentration will rise. Once a particular threshold is achieved, the concentration may become sufficient to increase cell renewal rates. It is also possible that these new factors alter the negative feedback of the system, allowing self-renewal rates to increase despite rising cell counts.

2.5 The Possibility of a Second Mutation

CML, as described above, results from a single mutation. A second mutation in which the new cells can produce their own growth factor could lead to the instability. Also, there has been some clinical evidence that in the late stages of CML, some of the stem cells lose their ability to differentiate properly [6]. This has led to the hypothesis that a second mutation occurs, leading to a new type of stem cell that does possess a growth advantage but cannot differentiate. As the reproductive system for stem cells is regulated via negative feedback loops, it will renew and differentiate more cells if the number of stem cells is small. Assuming this feedback system cannot recognize this second mutant as a stem cell, its presence would reduce the number of recognized stem cells. Hence, this would trigger greater production and differentiation via the negative feedback loop. This phenomenon could also lead to the instability.

Chapter 3

Mathematical Model

3.1 Approach and Assumptions

We will model the population dynamics of the various biological entities involved in the system. Initially, we will ignore the possibility of a second mutation and will use a very simple model for stem cell growth. Our initial model will involve coupled ordinary differential equations for the populations of:

- S, normal stem cells, and

- A, abnormal stem cells.

As we find results at this basic level that make sense and we feel comfortable with the dynamics between the entities modelled, we will slowly add on layers of complexity including a more realistic model for stem cell reproduction and regulation (called the G_0 model), time delays, the immune response, etc.

3.2 Logistic Growth Model

We start with a logistic growth model for the normal stem cell population. We denote the specific growth rate (net of cellular death during the reproductive cycle[1]), λ_s, and will write the proliferative limit, which relies on the total (normal and abnormal) stem cell population, as A_p. Denoting the normal stem cell population as S, we have

$$\dot{S} = \lambda_s S(1 - \frac{gS + A}{A_p}) - \mu_s S, \tag{3.1}$$

where μ_s is the rate of cellular differentiation (combined with the very small cellular death rate). The factor g allows for the possibility that the abnormal cells are less

[1]This type of cellular death is called apoptosis.

sensitive to the standard proliferative limit, A_p, than the normal stem cells. This may be used to represent the possibility that they do not rely on their own stem cell niche (if they produce their own growth factor, say), or that they are able to occupy some sort of physical or physiological niche that the normal cells cannot. Here, an analogy is useful to more clearly explain the factor g. Imagine either the stem cell niches or the actual physical spaces occupied by these cells as a hallway of hotel rooms. The normal stem cells, S, may only be allowed to occupy the rooms on the northern half of the hallway, while the abnormal cells, A, may check-in to any room they like. In this case, the factor g would be two because it would take two abnormal cells, on average, to occupy one room suitable for a normal cell. Clearly, to reflect this advantage, the factor g will always be greater than or equal to one.

The abnormal cells will satisfy

$$\dot{A} = \lambda_a A(1 - \frac{S + A}{A_p}) - \mu_a A - \beta_{ta} T A, \tag{3.2}$$

where the additional decay term stems from the immune response of active T cells (denoted by T). They will kill the abnormal cells at a rate governed by the law of mass action (represented by β_{ta}). One notes that the proliferative limit term does not have the factor g from equation 3.1 for the normal cell population. This is because the spaces available to normal stem cells form a subset of those available to the abnormal cells. Hence, both types of stem cells contribute equally to the filling of the total spaces available to the abnormal cells.

We start our analysis with the simplest versions of 3.1 and 3.2:

$$\dot{S} = \lambda_s S(1 - \frac{gS + A}{A_p}) - \mu S, \tag{3.3}$$

and

$$\dot{A} = \lambda_a A(1 - \frac{S + A}{A_p}) - \mu A. \tag{3.4}$$

3.2.1 Nondimensionalization

The first step in our analysis is to nondimensionalize the system. We write,

$$S = S^* A_p, \quad A = A^* A_p, \quad t = \frac{t^*}{\lambda_s}, \quad q = \frac{\mu}{\lambda_s}, \quad \rho = \frac{\lambda_a}{\lambda_s} \tag{3.5}$$

and substitute in the dimensionless variables yielding,

$$\dot{S} = S(1 - gS - A - q), \tag{3.6}$$

and

$$\dot{A} = \rho A(1 - S - A - q). \tag{3.7}$$

3.2.2 Steady States and Phase Plane Analysis

Next, we look at solutions to the equations where $\dot{S}$ and $\dot{A}$ are equal to zero. Clearly, the trivial solution (S,A)=(0,0) is one steady state. Also, it is easily verified that other steady states are:

$$S = \frac{1-q}{g},\ A = 0 \quad and \quad S = 0,\ A = 1 - q. \tag{3.8}$$

A steady state with positive values for both S and A only exists if the parameter $g = 1$. In this situation, a steady continuum exists along the line

$$S + A = 1 - q \tag{3.9}$$

for positive S and A.

To analyze the stability of these points, we consider the following phase plane plot. First, we consider the case with $g = 1$. This phase plane is shown in figure 3.1.

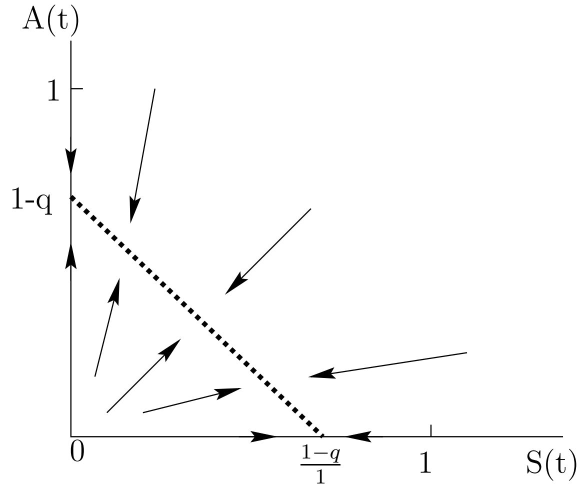

Figure 3.1: This phase plane demonstrates that for $g = 1$, there is a stable steady continuum connecting (1-q,0) and (0,1-q)

Clearly, all points on the phase plane other than the steady states form a basin of attraction to the steady continuum connecting the points (1-q, 0) and (0, 1-q).

As such, we see that the trivial steady state is unstable, while the non-trivial steady states are stable. This phase plane means very little, though, because with $g = 1$, the abnormal cells have no growth advantage. The phase plane in figure 3.2 has $g > 1$.

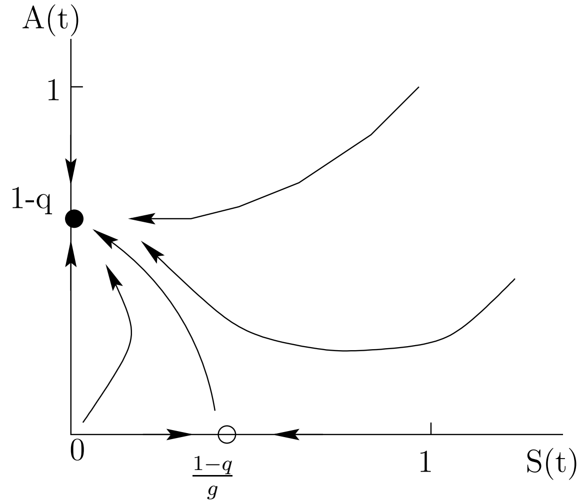

Figure 3.2: This phase plane demonstrates that for $g = 2$, the only stable steady state is at (0,1-q)

Now we have two non-trivial steady states: one case when all cells are abnormal and one when all cells are normal. This phase plane shows that, other than the steady states, the entire plane is a basin of attraction for the steady state at (0, 1-q). Hence, the state where the only remaining cells are abnormal is the only steady state. A slight perturbation from any steady state will lead to this stable point.

We now make the model slightly more complex model by allowing the normal and abnormal cells to have different differentiation and death parameters, μ_s and μ_a, respectively. We nondimensionalize the equations identically as done in 3.5 except that we introduce $q_s = \frac{\mu_s}{\lambda_s}$ and $q_a = \frac{\mu_a}{\lambda_s}$. This gives us the nondimensional equations

$$\dot{S} = S(1 - gS - A - q_s), \tag{3.10}$$

and

$$\dot{A} = \rho A(1 - S - A - q_a). \tag{3.11}$$

Following exactly as above, we find that the trivial solution is still a steady state. Similarly, we find the two other steady states:

$$S = \frac{1 - q_s}{g}, \; A = 0 \quad and \quad S = 0, \; A = 1 - q_a. \tag{3.12}$$

Unlike the first model, though, there may exist a third non-trivial steady state with positive values for both A and S, even with the parameter $g > 1$. Solving for this steady state, we find that

$$S^* = \frac{q_a - q_s}{g - 1}, \; A^* = 1 - q_a - \frac{q_a - q_s}{g - 1}, \tag{3.13}$$

To simplify further notation, we will call $S_0^a = \frac{1-q_s}{g}$ and $A_0^a = 1 - q_a$, which allows us to write the steady state values as

$$S^* = (\frac{g}{g-1})(S_0^a - \frac{A_0^a}{g}), \quad A^* = (\frac{g}{g-1})(A_0^a - S_0^a), \tag{3.14}$$

which will involve positive quantities for S and A if and only if,

$$q_s < q_a < \frac{g - 1 + q_s}{g}, \quad \textit{or equivalently}, \quad \frac{A_0^a}{g} < S_0^a < A_0^a. \tag{3.15}$$

These inequality are both shown in figure 3.3, where the shaded regions of the parameter spaces are the regions where there will be a steady state with positive normal and abnormal cell populations.

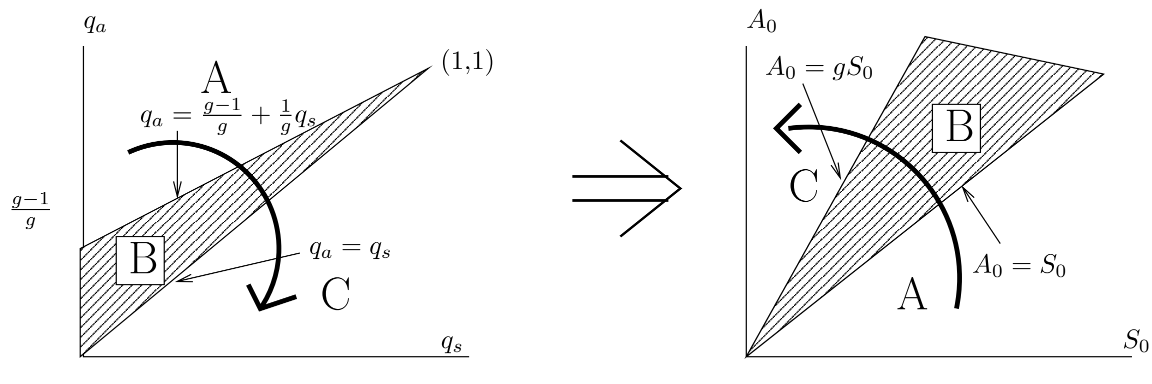

Figure 3.3: Parameter Space (q_s, q_a and S_0^a, A_0^a) Determining the Existence of Two Non-Trivial Equilibrium Populations

While the q_s, q_a parameter space is more useful in this very simple model, the S_0^a, A_0^a parameter space is included as it will be useful for comparisons with later, more complex models. A simple change of variables from one of these parameter spaces to the other makes it clear that the boundary $q_s = q_a$ is equivalent to the boundary $A_0^a = gS_0^a$, and the boundary $q_a = \frac{g-1+q_s}{g}$ is equivalent to to the boundary $A_0^a = S_0^a$. Thus, as we move clockwise from region A, through the shaded region B, to region C in the q_s, q_a space, we are moving counter-clockwise through A_0^a, S_0^a space. In figure 3.3, this is illustrated with the corresponding region labels and arrows.

Now, maintaining the abnormal niche and size advantage by keeping $g = 2$, we consider the three different A,S phase planes corresponding to the three regions of the q_s, q_a parameter space in figure 3.3. We only consider $q_s, q_a \in (0, 1)$ as these are the only values leading to positive steady states. As we see in figure 3.4, there is only one stable non-trivial steady state for each region in the space. Parameters in region A lead to the stability of the state with only normal cells, parameters in region B lead to the existence and stability of the steady state with positive normal and abnormal populations, and parameters in region C lead to the stability of the steady state with only abnormal cells.

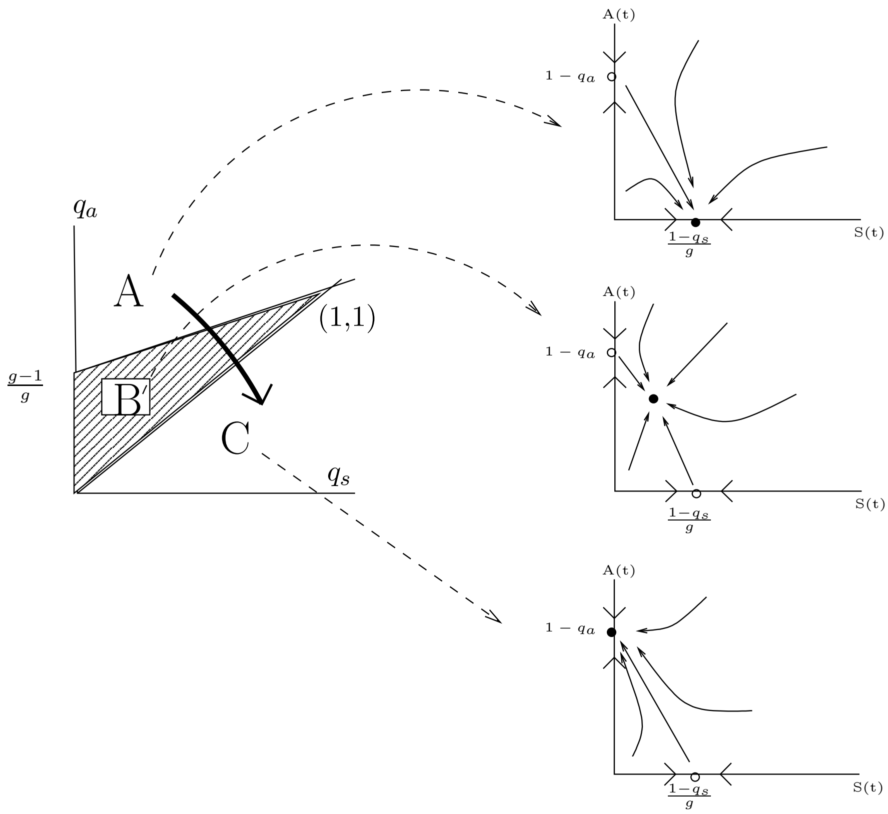

Figure 3.4: In this figure, we see how depending on which region of the parameter space the system is in, a different stable equilibrium state will emerge.

Hence, the entire phase plane will be a basin of attraction for one of the three steady states, depending exclusively on where the system is located in the parameter space.

3.2.3 Transcritical Bifurcations

As we cross the boundary from region A to region B, two equilibrium points will collide at $S = \frac{1-q_s}{g}$, $A = 0$ and produce a bifurcation called a transcritical bifurcation.

Whereas the phase plane in region A is such that this steady state is stable and all trajectories lead to it, the transcritical bifurcation leaves this state unstable while making the new non-trivial steady state stable. Then, this steady state will migrate from values of only normal cells, through combinations of normal and abnormals cells, and toward the value of only abnormal cells. When it reaches this point, it will collide with the other steady state at $S = 0, A = 1 - q_a$, causing another transcritical bifurcation that will leave this point stable. Hence, once we have passed through the parameter space to region C, all trajectories will lead to the state with only abnormal cells. These transcritical bifurcations are illustrated in figure 3.5.

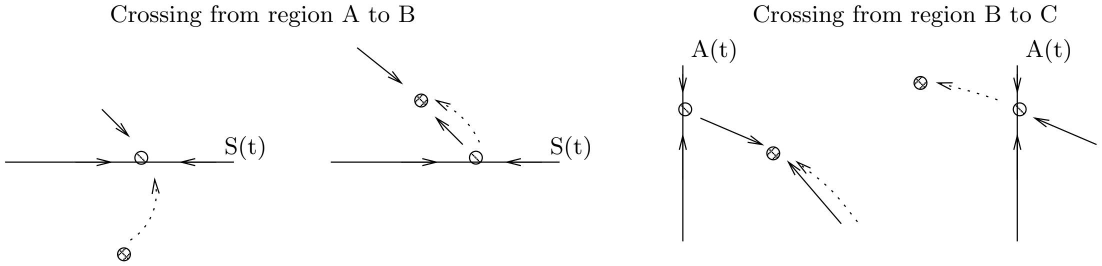

Figure 3.5: Illustration of the transcritical bifurcations ocurring at as we cross the boundaries first from region A to B and then from region B to C. The dotted arrows indicate the direction of the third steady state as it moves through the parameter space. The solid arrows point toward the stable steady state.

3.3 The G_0 Stem Cell Model

The preceding analysis is a nice starting point, but we would like to model more realistically the way in which stem cells develop. In normal tissue, stem cells progress through a multi-staged system. At each stage or compartment, cells may be involved in one of three activities. They may remain "resting" in the so-called G_0 phase. In this phase, the cells neither proliferate nor initiate any further cellular differentiation and remain in their current compartment.

Alternatively, they may begin a self-renewal process (at a rate $\beta(S)$) involving four phases. The first, called the G_1 phase, is the first "Gap" (hence the "G") in the reproductive process before DNA synthesis (S). While in this phase, the cell is busy producing cell components that will be required by the daughter cells resulting from the reproductive cell cycle. After Gap1, the cell enters the synthesis phase and the new DNA, as well as a number of proteins, are synthesized. During synthesis, the chromosomal DNA is copied into two sister chromatids. After synthesis, the cell enters another gap phase, called G_2 or Gap2, during which more proteins are produced, the material used for the cell membrane is created, and chromosomes are formed by the supercoiling of the DNA. Finally, the cell moves on to mitosis (M), during which the cell will actually divide into two daughter cells. Each daughter cell is given one of the two sister chromatids formed earlier, during DNA synthesis. Hence, after a time delay t_0, two cells re-enter the compartment as a result of one cell self-renewing. Some cells will die (at a rate a) during this proliferation process. This type of cellular death is called apoptosis.

Finally, the third possibility is that the cells leave a given compartment (at a rate $\delta(S)$) and begin the process of cellular differentiation. In normal healthy tissue, each stem cell will, on average, give rise to one G_0 state stem cell and one differentiating cell, which will continue on to several further compartments. This model [26] is known as the G_0 model and is illustrated in figure 3.6.

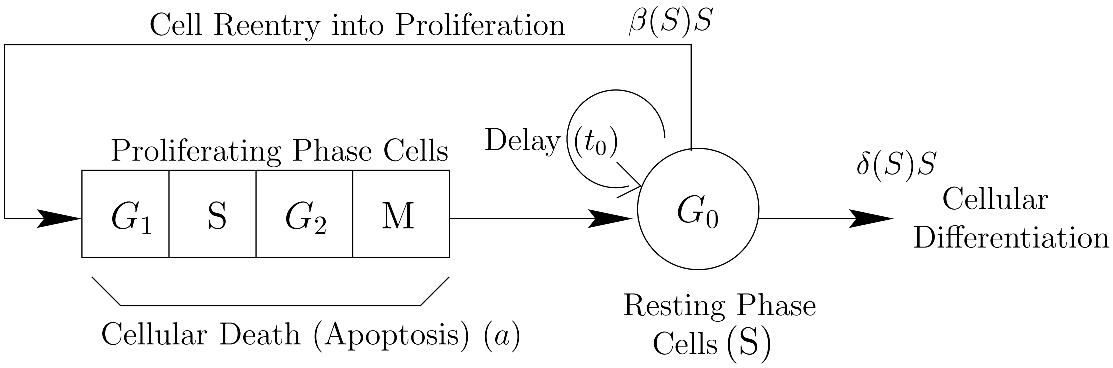

Figure 3.6: The G_0 Model for stem cell growth illustrates how cells may either remain in the G_0 resting phase, begin to differentiate into different types of cells, or reproduce. Reproduction is a four stage process beginning with the Gap1 phase (G_1), moving to DNA Synthesis (S), the second gap phase (G_2), and finally, mitosis (M).

As stem cells progress to the further compartments and head toward the later stages of differentiation, the probability of self-renewal decreases and this naturally increases the relative chance of further movement toward differentiation. Control over the self-renewal and differentiation processes is exercised through negative feedback loops - a very common biological regulatory mechanism. This control is most likely implemented independently at each compartment in the stem cells' life cycle.

In CML, the abnormal stem cell population dominates that of the normal stem cells. However, clinical research [4] has shown that the ratio of abnormal stem cells to normal stem cells is markedly lower (perhaps as low as 1:1) in the more primitive compartments compared with the later stages of development toward differentiation (perhaps as high as 1000:1, but generally around 100:1). This is shown in figure 3.7.

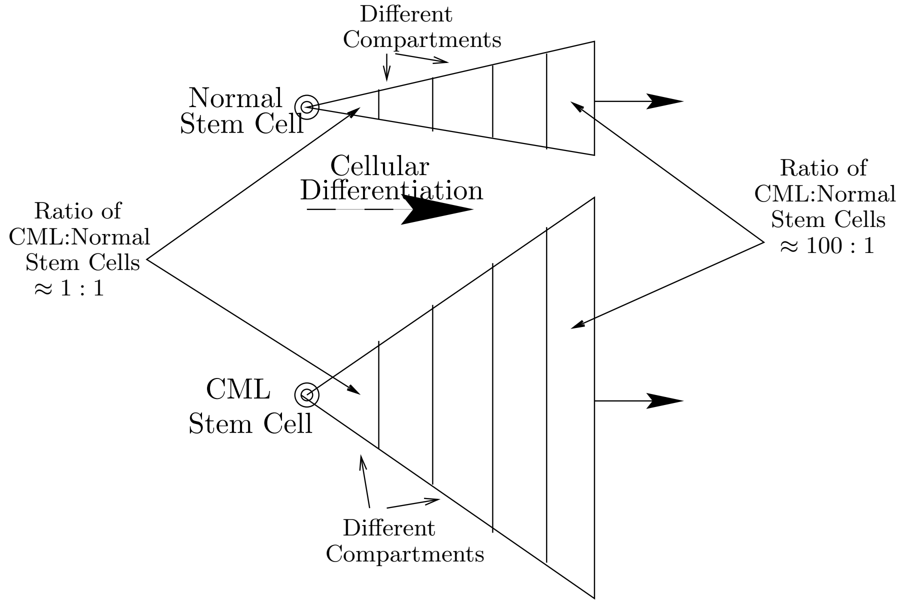

Figure 3.7: Comparison of Normal vs. CML Stem Cell Progression: Though the ratio of abnormal to normal stem cells may be relatively small in the early "compartments," this ratio steadily rises as the cells move toward differentiation. To incorporate this, a model would have to be age dependent.

Though the parameters and characteristics of the G_0 model change from one compartment to the next, it would be too complex to build an age dependent model. Hence, we will simplify the compartment system and assume that we can represent the stem cell's lifespan as one cycle, or compartment, of the G_0 model. Hence, once a cell undergoes differentiation, we assume it loses its "stemness" and is no longer a part of the stem cell population. As such, our parameter values for processes such as differentiation will be significantly smaller than the values for any specific compartment, as our value represents the product of all the compartments' respective differentiation rates.

3.4 Single Population

If we consider the total amount of cells resting in the G_0 phase to be the population of stem cells, we see from figure 3.6 that

$$\dot{S} = S(t-t_0)\beta(S(t-t_0))2(1-a) - S(t)(\beta(S(t)) + \delta(S)). \tag{3.16}$$

Comparing this equation with 3.3, we note that they would be very similar if we set the function $\beta(S)$ equal to the logistic growth function. This, however, would allow the rate of self-renewal to be negative - a clear inconsistency with the biological reality. In order to maintain the negative feedback properties of the logistic growth model while ensuring that the self-renewal rate remains non-negative, we define

$$\beta(S) = \frac{\lambda_s}{1 + (\frac{S}{S_p})^2}, \tag{3.17}$$

where S_p is the proliferative limit parameter for S.

Substituting 3.17 into 3.16 and writing $S(t - t_0)$ as S_{t_0}, we get

$$\dot{S} = 2(1-a)\frac{S_{t_0}\lambda_s}{1 + (\frac{S_{t_0}}{S_p})^2} - \frac{S\lambda_s}{1 + (\frac{S}{S_p})^2} - \delta S, \tag{3.18}$$

where we have assumed that δ is a constant differentiation rate.

We nondimensionalize 3.18 in the same way as for the logistic model and define the nondimensional delay parameter, $\tau = t_0\lambda_s$, yielding

$$\dot{S} = 2(1-a)\frac{S_\tau}{1 + S_\tau^2} - \frac{S}{1 + S^2} - qS, \tag{3.19}$$

where $q = \frac{\delta}{\lambda_s}$. From this equation, we see that the only positive non-trivial steady state is

$$S^* = \sqrt{\frac{1 - 2a - q}{q}}. \tag{3.20}$$

To make the notation easier, we now rewrite 3.19 as

$$\dot{S} = R(S_\tau) - D(S) \tag{3.21}$$

where $R(S) = 2(1-a)\frac{S}{1+S^2}$ and $D(S) = \frac{S}{1+S^2} + qS$.

3.4.1 Linear Stability

We start with the nonlinear evolution equation 3.21 where both R and D are nonlinear functions. From 3.20, we know that $R(S^*) - D(S^*) = 0$. We are interested in studying the evolution of perturbations to the steady state $S = S^*$. We write

$$S = S^* + s(t), \tag{3.22}$$

which leads to the nonlinear equations for $s(t)$,

$$\dot{s} = \Big(R(S^* + s(t-\tau)) - D(S^* + s(t))\Big) - \Big(R(S^*) - D(S^*)\Big). \tag{3.23}$$

An analysis of linear stability relies on the assumption that the perturbation, s, from the steady state is small and hence, it is reasonable to linearize equation 3.23. To do this, we write the Taylor series expansion of the nonlinear operators R and D as a series in s to get

$$R(S^* + s(t-\tau)) - D(S^* + s(t)) = (R(S^*) - D(S^*)) + \mathcal{L}(S^*)s + O(s^2), \quad (3.24)$$

where $\mathcal{L}(S^*)$ is a linear operator acting on s, called the Fréchet derivative of $R - D$. Since s is small, we may ignore the quadratic terms in s and hence have the linear equation

$$\dot{s} = \mathcal{L}s \approx R'(S^*)s(t-\tau) - D'(S^*)s(t). \quad (3.25)$$

We assume that $s(t) = e^{\sigma t}$ and see that,

$$\sigma \approx R'(S^*)e^{-\sigma\tau} - D'(S^*). \quad (3.26)$$

We substitute $\lambda = \sigma\tau$ to give

$$\frac{\lambda}{\tau} = R'(S^*)e^{-\lambda} - D'(S^*). \quad (3.27)$$

Let

$$\mu = \tau R'(S^*) \quad (3.28)$$

and

$$\nu = \tau D'(S^*), \quad (3.29)$$

and hence,

$$\lambda = \mu e^{-\lambda} - \nu. \quad (3.30)$$

Since the perturbation from the steady state is of the form $e^{\sigma t}$, we seek to determine if there are conditions under which the real part of σ, and equivalently the real part of λ, is positive. If this were to occur, then the perturbation would grow, leaving the steady state linearly unstable. We separate the real and imaginary parts by putting $\lambda = \gamma + i\omega$ and substituting into 3.30. This gives, for the real and imaginary parts,

$$\gamma = \mu e^{-\gamma} \cos\omega - \nu, \tag{3.31}$$

and

$$\omega = -\mu e^{-\gamma} \sin\omega. \tag{3.32}$$

If we suppose that $\gamma > 0$, then $e^{-\gamma} < 1$. Hence,

$$\gamma < |\mu| - \nu. \tag{3.33}$$

If we consider $\nu > 0$, we see that to avoid contradiction with our assumption that $\gamma > 0$, we must have $|\mu| > \nu$. Hence, we conclude that $Re\ \lambda \leq 0$ for

$$|\mu| \leq \nu. \tag{3.34}$$

We treat μ as a bifurcation parameter. As γ varies continuously, if we get instability with increasing $|\mu|$, then $\gamma = 0$ at the critical value, and this leads to the conditions

$$\nu = \mu \cos\omega, \tag{3.35}$$

and

$$\omega = -\mu \sin\omega. \tag{3.36}$$

Equations 3.35 and 3.36 determine μ through

$$\mu = \nu \sec\omega, \tag{3.37}$$

where ω is a solution to

$$\omega = -\nu \tan\omega. \tag{3.38}$$

Following Andrew Fowler's book [13], we find the infinite number of roots of 3.38 graphically. As shown in figure 3.8, each intersection of $\tan\omega$ and $-\frac{\omega}{\nu}$ is a root to 3.38. It is clear that the first solution is $\omega = 0$, which corresponds to the case where $\sigma \in \Re$. In this single population case, however, there is only one non-trivial steady state and hence, we are not interested in a real σ as this generally corresponds to a saddle-node transition.[2] However, if σ is complex and its real part is greater than zero, then it will oscillate with increasing amplitudes. Each of the infinite solutions

[2]This case will be relevant when we reach the two population system.

to 3.38 will represent a bifurcation to a different type of instability. We will only concern ourselves, though, with the smallest non-zero solution for ω because for this single population case, we are interested in the first onset of oscillatory instability. As $\nu \geq 0$, we see that the first positive solution, ω^+ will lie between $\frac{\pi}{2}$ and π.[3]

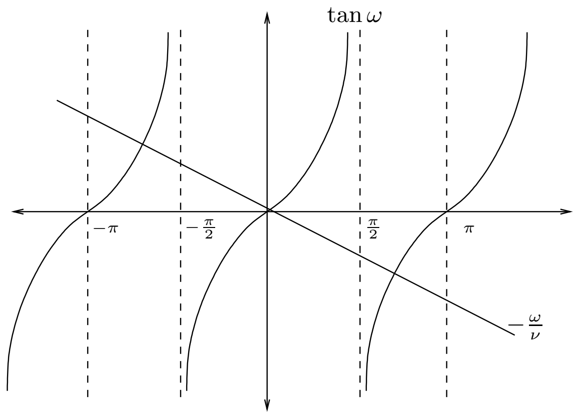

Figure 3.8: The roots to 3.38 shown graphically

One can code a short program[4] using the scalar iteration

$$\omega_{n+1} = \tan^{-1}(-\frac{\omega_n}{\nu}) + \pi \tag{3.39}$$

to find and plot the solution for ω^+ as ν varies. As we are searching specifically for a solution $\omega^+ \in (\frac{\pi}{2}, \pi)$, we choose $\omega_0 = \frac{3\pi}{4}$ and we add a π term as the arctangent function has a range of $(-\frac{\pi}{2}, \frac{\pi}{2})$. This plot is shown in figure 3.9.

For each ν, once a value of ω is obtained, one may plot the corresponding value for μ using the relationship in equation 3.37. Figure 3.10 shows the corresponding plot for μ as a function of ν.

From 3.34, we know we have stability when $|\mu| \leq \nu$. We also know that moving downward from this region of stability, the solution remains stable until it reaches the bottom line generated from 3.37. Hence, the region below this bifurcation line is the space where the steady state gives rise to oscillatory instability.

3.5 Populations of Normal and Abnormal Stem Cells

Now we seek to add the population of abnormal stem cells to the model and see how the system is affected. The G_0 model for the stem cells will be very similar to 3.18,

[3]Similarly, we see that the first negative solution, ω^- is simply $-\omega^+$.

[4]See Appendix A for code.

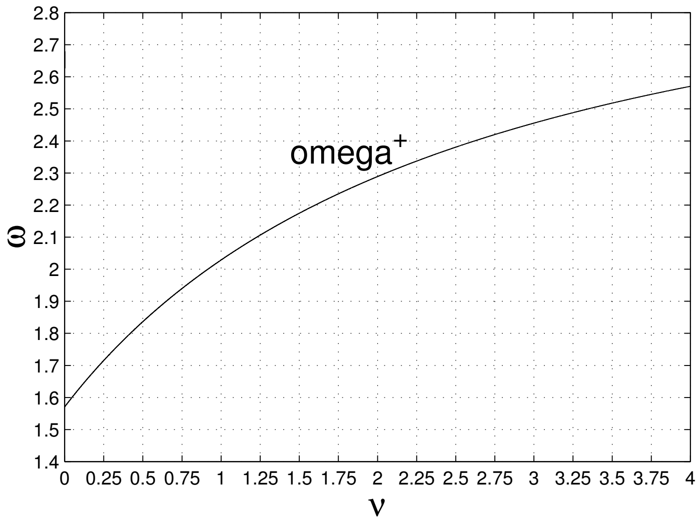

Figure 3.9: The numerical solutions for ω^+ and ω^- verses ν.

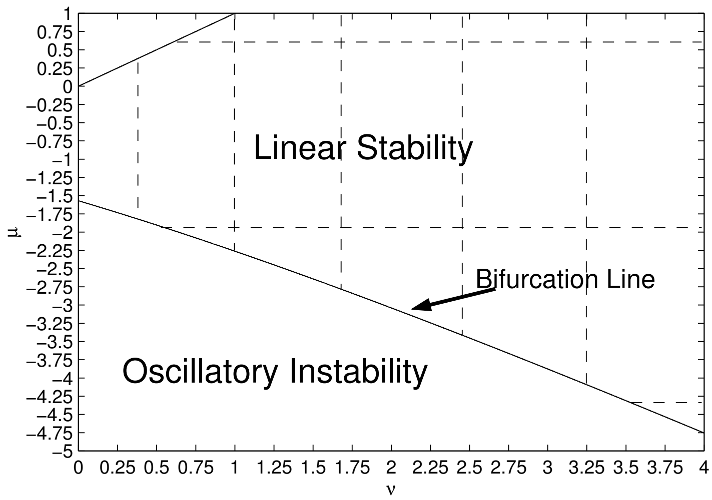

Figure 3.10: A plot of the stability region defined by $|\mu| \leq \nu$ and the line representing the bifurcation to instability

except that there will be two different time scales (λ_s and λ_a), differentiation rates (δ_s and δ_a), and apoptosis rates (a and b) for the normal and abnormal cells, respectively. In addition, the negative feedback mechanism in the β-function will be that which we used in the logistic growth model for the two populations. Hence, we have

$$\dot{S} = 2(1-a)\frac{S_{t_0}\lambda_s}{1+(\frac{gS_{t_0}+A_{t_0}}{A_p})^2} - \frac{S\lambda_s}{1+(\frac{gS+A}{A_p})^2} - S\delta_s, \tag{3.40}$$

and

$$\dot{A} = 2(1-b)\frac{A_{t_0}\lambda_a}{1+(\frac{S_{t_0}+A_{t_0}}{A_p})^2} - \frac{A\lambda_a}{1+(\frac{S+A}{A_p})^2} - A\delta_a. \tag{3.41}$$

We nondimensionalize the system in the same way as we did for the logistic model to get

$$\dot{S} = 2(1-a)\frac{S_\tau}{1+(gS_\tau + A_\tau)^2} - \frac{S}{1+(gS+A)^2} - q_s S \tag{3.42}$$

where $q_s = \frac{\delta_s}{\lambda_s}$, and

$$\dot{A} = 2(1-b)\rho\frac{A_\tau}{1+(S_\tau + A_\tau)^2} - \rho\frac{A}{1+(S+A)^2} - q_a A \tag{3.43}$$

where $\rho = \frac{\lambda_a}{\lambda_s}$, and $q_a = \frac{\delta_a}{\lambda_s}$.

3.5.1 Steady States

First, we look for steady states. It is clear that the trivial steady state, (S,A)=(0,0), exists, and we can also easily see that steady states will exist in the two cases where there are no abnormal cells, A, but a positive amount of normal cells, S, and vice-versa. We start by solving for these points.

We set 3.42 equal to zero and solve for the case where $A = 0$ to find the steady state,

$$S^* = \sqrt{\frac{1-2a-q_s}{g^2 q_s}}, \quad A^* = 0. \tag{3.44}$$

Similarly, setting 3.43 equal to zero and solving with S=0, we find the steady state,

$$A^* = \sqrt{\frac{(1-2b)\rho - q_a}{q_a}}, \quad S^* = 0. \tag{3.45}$$

Now, we are interested in finding whether a steady state exists with non-trivial, positive values for both S and A. First solving for positive A, under the assumption that $g > 1$, we find that

$$A^* = \left(\sqrt{\frac{(1-2b)\rho - q_a}{q_a}} - \sqrt{\frac{1-2a-q_s}{g^2 q_s}}\right)\left(\frac{g}{g-1}\right), \tag{3.46}$$

and then solving for S, one finds

$$S^* = \left(\sqrt{\frac{1-2a-q_s}{g^2 q_s}} - \frac{1}{g}\sqrt{\frac{(1-2b)\rho - q_a}{q_a}}\right)\left(\frac{g}{1-g}\right). \tag{3.47}$$

Here, it is natural to refer to the analysis of the logistic growth model in section 3.2. We note the fact that expressions 3.46 and 3.47 have similar terms and these terms are indeed the single population abnormal and normal equilibrium levels respectively. Just as we did in section 3.2, we write them with the variables

$$S_0^b = \sqrt{\frac{1-2a-q_s}{g^2 q_s}} \tag{3.48}$$

and

$$A_0^b = \sqrt{\frac{(1-2b)\rho - q_a}{q_a}}, \tag{3.49}$$

to give the steady state,

$$S^* = (\frac{g}{g-1})(S_0^b - \frac{A_0^b}{g}), \quad A^* = (\frac{g}{g-1})(A_0^b - S_0^b). \tag{3.50}$$

Since we know that the parameter $g > 1$, we know that our steady state will involve positive values of normal and abnormal cells if and only if

$$\frac{A_0^b}{g} < S_0^b < A_0^b. \tag{3.51}$$

This relationship is identical to that in the logistic growth model and is seen graphically in figure 3.11, where the shaded region represents the parameter space where there will exist a steady state with positive values of S and A.

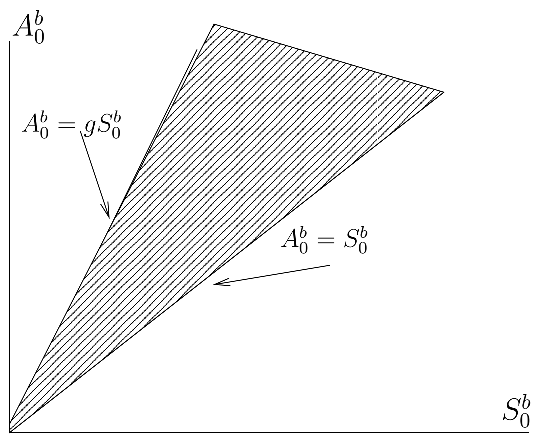

Figure 3.11: Parameter Space (S_0^b, A_0^b) Determining the Existence of Two Non-Trivial Equilibrium Populations

3.5.2 Linear Stability

Using the same type of notation as in the single population case, we rewrite 3.42 as

$$\dot{S} = R_1(S_\tau, A_\tau; g, a) - D_1(S, A; g, q_s), \tag{3.52}$$

where $R_1(S,A) = 2(1-a)\frac{S}{1+(gS+A)^2}$ and $D_1(S,A) = \frac{S}{1+(gS+A)^2} + q_s S$, and we rewrite 3.43 as

$$\dot{A} = R_2(S_\tau, A_\tau; \rho, b) - D_2(S, A; \rho, q_a), \tag{3.53}$$

where $R_2(S,A) = 2(1-b)\rho\frac{A}{1+(S+A)^2}$ and $D_2(S,A) = \rho\frac{A}{1+(S+A)^2} + q_a A$.

As in our analysis of the single population model, we linearize about the steady states. Before the first mutation in the stem cells occurs, the body will achieve a steady state with a positive amount of normal cells and no abnormal cells.

Steady State with $S > 0$ and $A = 0$

Hence, we start by looking at the steady state defined in 3.44 by writing

$$S = S^* + e^{\sigma t} \tag{3.54}$$

and

$$A = 0 + Ce^{\sigma t}. \tag{3.55}$$

Following identically as in the linear stability analysis in subsection 3.4.1, we see

$$\dot{s} = \Big(\frac{dR_1}{dS}(S^*,0) + C\frac{dR_1}{dA}(S^*,0)\Big)s(t-\tau) - \Big(\frac{dD_1}{dS}(S^*,0) + C\frac{dD_1}{dA}(S^*,0)\Big)s(t). \tag{3.56}$$

And again setting $s(t) = e^{\sigma t}$, we see that

$$\sigma \approx \Big(\frac{dR_1}{dS}(S^*,0) + C\frac{dR_1}{dA}(S^*,0)\Big)e^{-\sigma\tau} - \Big(\frac{dD_1}{dS}(S^*,0) + C\frac{dD_1}{dA}(S^*,0)\Big). \tag{3.57}$$

In the exact same manner as done above to find 3.57 from 3.52 and 3.54, we can use 3.53 and 3.55 to find that

$$C\sigma \approx \Big(\frac{dR_2}{dS}(S^*,0) + C\frac{dR_2}{dA}(S^*,0)\Big)e^{-\sigma\tau} - \Big(\frac{dD_2}{dS}(S^*,0) + C\frac{dD_2}{dA}(S^*,0)\Big). \tag{3.58}$$

To simplify notation, we write $\alpha_1 = \frac{dR_1}{dS}(S^*,0)$, $\beta_1 = \frac{dR_1}{dA}(S^*,0)$, $p_1 = \frac{dD_1}{dS}(S^*,0)$, $q_1 = \frac{dD_1}{dA}(S^*,0)$, $\alpha_2 = \frac{dR_2}{dS}(S^*,0)$, $\beta_2 = \frac{dR_2}{dA}(S^*,0)$, $p_2 = \frac{dD_2}{dS}(S^*,0)$, and $q_2 = \frac{dD_2}{dA}(S^*,0)$.

Here, we note that $R_2(S,A) = A \times F_1(S,A)$ and $D_2(S,A) = A \times F_2(S,A)$ for some functions F_1 and F_2. Keeping this notation, we may write

$$\alpha_2 = \frac{dR_2}{dS} = A\frac{dF_1}{dS} \tag{3.59}$$

and

$$p_2 = \frac{dD_2}{dS} = A\frac{dF_2}{dS}. \tag{3.60}$$

Clearly, when one evaluates equations 3.59 and 3.60 at the point $(S^*, 0)$, they will be equal to zero. Hence, equation 3.58 can be written as

$$C\sigma = C\beta_2 e^{-\sigma\tau} - Cq_2. \tag{3.61}$$

Now we have a system of two equations, 3.57 and 3.61, that will determine C and σ. We start with the assumption that $C \neq 0$. This assumption means that if there is instability, it will emerge at both the $A = 0$ steady state as well as the $S = S^*$ steady state. This immediately raises concerns because if this instability is oscillatory instability, it implies that the A level might become negative, which would clearly be biologically impossible. However, it can be shown using equation 3.53 that if A is initially zero and at some later time there is a perturbation to a positive level, the abnormal population will never reach a negative value.[5] This implies that, should we find an oscillatory instability from this point, it would presumably involve an oscillation around a positive drift (due to a real eigenvalue).

Now, we can reduce 3.61 to

$$\sigma = \beta_2 e^{-\sigma\tau} - q_2, \tag{3.62}$$

which can be treated identically as equation 3.26. We make the substitution $\lambda = \sigma\tau$, define

[5] We start with $\dot{A} = R_2(A_\tau) - D_2(A)$. We assume that $A = 0\ \forall\ t < 0$ and that $A(0) > 0$. Our aim is to show that $A \geq 0\ \forall\ t > 0$. A is piecewise continuous and its only discontinuity lies at 0. We let $t = T > 0$ be the first time after the discontinuity that $A = 0$. Thus, $A \geq 0\ \forall\ t \leq T$. We know that $D_2(0) = 0$, and since $R_2(A) \geq 0$ when $A \geq 0$, we have $\dot{A}(T) = R_2(A(T-\tau)) \geq 0$. However, if $\dot{A} > 0$ at the point $A(T) = 0$, this would necessarily imply that $A < 0$ for $t < T$, which is a contradiction. Hence, we know that $R_2(A(T-\tau)) = 0$, which implies that $A(T-\tau) = 0$. But, since $A(0) > 0$, and A is continuous, this implies that $T < \tau$. Therefore, for $t \in (0,T)$, $\dot{A} = -D_2(A)$. This differential equation is in quadrature form and integrating it yields $t = \int_A^{A(0)} \frac{dA}{D_2(A)}$. Since $D_2(A) > 0$ and $D_2 \sim A$ as $A \to 0$, this implies that it will take infinite time to reach $A = 0$ and thus, $A > 0$ for $t \in (0,\tau)$. This gives us the required contradiction and therefore, we have shown that $A \geq 0\ \forall\ t$ (and in fact $A > 0\ \forall\ t$). For more rigorous examination of similar and more general cases, see Gyori and Ladas [16].

$$\mu_1 = \tau\beta_2 \tag{3.63}$$

and

$$\nu_1 = \tau q_2, \tag{3.64}$$

and then proceed identically as we did with equation 3.30 for the single population case. As these cases are identical (in μ,ν space), we will have the same region where we know there is stability,

$$|\mu_1| \leq \nu_1, \tag{3.65}$$

as well as the same bifurcation line as shown in figure 3.10. Again, this means that in the parameter space just above the bifurcation line, we will have linear stability, while below the line, there will be oscillatory instability. Finally, we return to equation 3.57 to find that non-zero C will satisfy

$$C = \frac{(\beta_2 - \alpha_1)e^{-\sigma\tau} + p_1 - q_2}{\beta_1 e^{-\sigma\tau} - q_1}. \tag{3.66}$$

Unlike the single population case, it is logical in this case to consider the bifurcation line beyond which perturbations will have a positive drift. As we saw in the logistic two population model, it is entirely feasible to have a saddle node, like the steady state involving only normal cells, that gives rise to non-oscillatory drift instabilities. In that case, when the abnormal cells had a growth advantage ($g > 1$), perturbations from that steady state grew exponentially, leading to a steady state involving only abnormal cells. In such a case, $\sigma \in \Re^+$. Since σ varies continuously with μ and ν, we know that this bifurcation will occur when $\sigma = 0$ which implies that $\mu_1 = \nu_1$. Hence, the region defined by $\mu_1 > \nu_1$ will involve an instability characterized by a drift away from the steady state. This more complete picture of the types of instability within the parameter space is given in figure 3.12.

Alternatively, we consider the case where the steady state $S = S^*$ becomes unstable, while the abnormal cell population's steady state does not. This means that $C = 0$, and equation 3.57 will reduce to

$$\sigma = \alpha_1 e^{-\sigma\tau} - p_1, \tag{3.67}$$

which will give us the same stability and bifurcation conditions as above. Hence, $|\mu_2| \leq \nu_2$ defines a stability region where

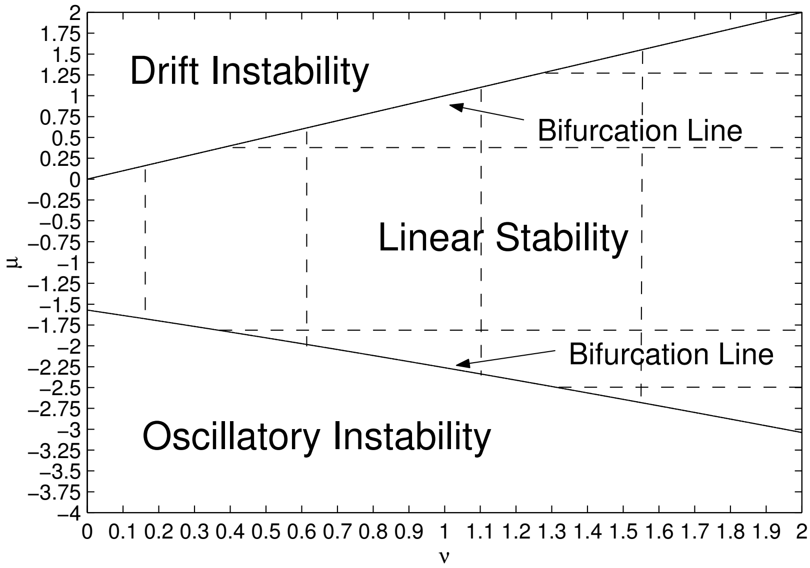

Figure 3.12: Parameter Space of Instabilities

$$\mu_2 = \tau\alpha_1 \tag{3.68}$$

and

$$\nu_2 = \tau p_1, \tag{3.69}$$

while the bifurcation lines drawn in figure 3.12 still hold (again, for these newly defined μ_2 and ν_2).

Steady State with $S = 0$ and $A > 0$

Now, we will examine the steady state defined in 3.45. We write

$$S = 0 + Ce^{\sigma t} \tag{3.70}$$

and

$$A = A^* + e^{\sigma t}. \tag{3.71}$$

Following exactly as we did for the first steady state, we find

$$C\sigma \approx (C\alpha_1 + \beta_1)e^{-\sigma\tau} - (Cp_1 + q_1), \tag{3.72}$$

and

$$\sigma \approx (C\alpha_2 + \beta_2)e^{-\sigma\tau} - (Cp_2 + q_2), \tag{3.73}$$

where we now evaluate the derivatives α_1, β_1, p_1, q_1, α_2, β_2, p_2, and q_2 at the point $(0, A^*)$ instead of at $(S^*, 0)$ as before.

Similar to the preceding case, $\beta_1 = 0$ and $q_1 = 0$ and hence equations 3.72 and 3.73 will determine C and σ. As before, we first examine the case where $C \neq 0$ and find the region $|\mu_3| \leq \nu_3$ to be stable where

$$\mu_3 = \tau\alpha_1 \tag{3.74}$$

and

$$\nu_3 = \tau p_1. \tag{3.75}$$

C is defined by

$$C = \frac{(\alpha_1 - \beta_2)e^{-\sigma\tau} - p_1 + q_2}{\alpha_2 e^{-\sigma\tau} - p_2}, \tag{3.76}$$

and the bifurcation diagram shown in 3.12 holds for the new definitions of μ_3 and ν_3.

For the case where $C = 0$, the region defined by $|\mu_4| \leq \nu_4$ is stable where

$$\mu_4 = \tau\beta_2 \tag{3.77}$$

and

$$\nu_4 = \tau q_2. \tag{3.78}$$

Again, the bifurcation lines to both oscillatory instability as well as to a drift instability both hold under these definitions.

Steady State with $S > 0$ and $A > 0$

Without Delay

Evaluation of the stability of the steady state $S = S^*$ and $A = A^*$ is far less trivial than the other two cases. As such, we first consider the system without a delay. To gain an initial concept of the nature and characteristics of this equilibrium point, we refer to the insight gained from our analysis of the third non-trivial steady state in the logistic model. We know that outside of the shaded region of the parameter space in figure 3.11, this steady state does not exist. It is reasonable to assume that the conclusions from our analysis of the logistic model will hold true for this more complex model and hence, that as we move from one boundary of the shaded region toward the other, this new steady state will pass through the positive A_0^b, S_0^b quadrant, starting from one of the steady states and ending at the other. Further, we saw in the logistic model that there were two transcritical bifurcations, one ocurring at each of these boundaries. First, we start with the rightmost boundary line $A_0^b = S_0^b$. If we evaluate the steady state defined in 3.50 on this line, we find that $A^* = 0$ and $S^* = S_0^b$. Next, we consider the left boundary line, $A_0^b = gS_0^b$. On this line, the steady state defined by equation 3.50 gives $A^* = gS_0^b = A_0^b$ and $S^* = 0$. Hence, we conclude that when moving counter-clockwise from the lower boundary of parameter space in figure 3.11 through the shaded region and to the upper boundary, the "third" non-trivial steady state moves from the one with all normal cells to the one with all abnormal cells. Indeed, this is identical to the case in the logistic model. This migration of the third steady state is shown in figure 3.13.

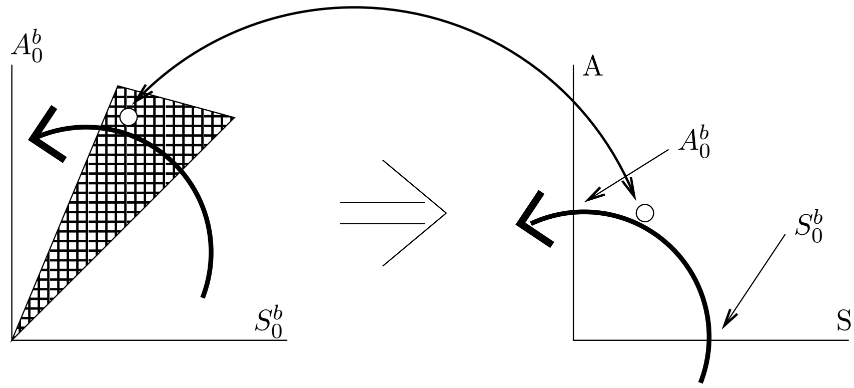

Figure 3.13: As one moves from right to left through the shaded region of the parameter space, the third non-trivial steady state moves through the phase plane from the state with all normal cells to the state with all abnormal cells

.

Also like the logistic case, the phase plane relies on where the system lies in the parameter space. For this steady state to exist, the parameters must lie within the shaded region, which leads to the stability of this steady state. When this point exists, the phase plane is identical to that corresponding to region B in figure 3.4.

With Delay

We add the delay term and proceed as we did for the other steady states. We write

$$S = S^* + Be^{\sigma t} \tag{3.79}$$

and

$$A = A^* + Ce^{\sigma t}. \tag{3.80}$$

As before, we linearize about the steady state and find,

$$B\sigma e^{\sigma t} \approx (B\alpha_1 + C\beta_1)e^{-\sigma\tau}e^{\sigma t} - (Bp_1 + Cq_1)e^{\sigma t}, \tag{3.81}$$

and

$$C\sigma e^{\sigma t} \approx (B\alpha_2 + C\beta_2)e^{-\sigma\tau}e^{\sigma t} - (Bp_2 + Cq_2)e^{\sigma t}, \tag{3.82}$$

where we now evaluate the derivatives α_1, β_1, p_1, q_1, α_2, β_2, p_2, and q_2 at the point (S^*, A^*). We put this system in matrix form and write

$$\begin{pmatrix} \sigma Be^{\sigma t} \\ \sigma Ce^{\sigma t} \end{pmatrix} = \begin{pmatrix} \alpha_1 e^{-\sigma\tau} - p_1 & \beta_1 e^{-\sigma\tau} - q_1 \\ \alpha_2 e^{-\sigma\tau} - p_2 & \beta_2 e^{-\sigma\tau} - q_2 \end{pmatrix} \begin{pmatrix} Be^{\sigma t} \\ Ce^{\sigma t} \end{pmatrix} = \mathcal{J} \begin{pmatrix} Be^{\sigma t} \\ Ce^{\sigma t} \end{pmatrix}, \tag{3.83}$$

where the $\mathcal{J}$ is the Jacobian matrix, and σ is an eigenvalue of $\mathcal{J}$. For stability to exist, the real portions of all of the eigenvalues must be less than or equal to zero. To solve for the eigenvalues of $\mathcal{J}$, we must solve for the roots of the characteristic polynomial

$$Det(\mathcal{J} - \sigma) = \sigma^2 - \sigma Tr(\mathcal{J}) + Det(\mathcal{J}) = 0, \tag{3.84}$$

where $Det(A)$ and $Tr(A)$ denote the determinant and trace of the matrix A. If one calculates the coefficients of the characteristic polynomial, they can solve for the conditions which would lead to instability using a number of techniques. However, the algebra involved in doing this analytically becomes too complicated for the purposes of this paper. In chapter 4, once we have substituted suitable parameter values into the equations, we will solve numerically for the coefficients of this characteristic polynomial. Then, we will try to determine if, for that given set of parameter values, there is a delay that would lead to instability.

Chapter 4

Numerical Analysis

4.1 Parameter Values

In this chapter, we will use the mathematical model developed in the previous chapter to determine numerical solutions for the populations of normal and abnormal cells. To do this, we must first find reasonable estimates for the values of the parameters. This is a very difficult task as biologists do not appear to have much data on the parameters in the G_0 model in humans. Many papers do address the parameter values in cats and mice, though many such studies make measurements from cell cultures grown in a lab, outside of the animals' bodies. *Here it must be emphasized that the parameter values used fall within the very wide confidence intervals offered by several different papers. Further, even if we assume that these broad confidence intervals are valid, it is unclear what the relationship is between the parameter values in mice and cats and those in humans.*

With this uncertainty in mind, we wish to examine our model using some sample parameters determined in these experiments. Michael Mackey gives the results of several trials aimed at determining the steady state values for many of these parameters [26]. Table 4.1 shows the results of Bradford, Cheshier, and Abkowitz [26] for the apoptosis rate (a), the reproduction rate (β), the differentiation rate (δ), and the delay time for reproduction (t_0).

Parameter	Bradford	Cheshier	Abkowitz
a (day^{-1})	0.069 (.200,0)	0.228 (.599,0)	0.007 (0,.071)
β (day^{-1})	0.020 (.031,.015)	0.053 (.077,.038)	0.057 (.022,.08)
δ (day^{-1}	0.010 (0,.015)	0.024 (0,.038)	0.042 (.011,.075)
t_0 (day)	4.25 (3.40,9.86)	1.41 (1.15,1.67)	

Table 4.1: Experimental Results for G_0 Model Parameters in Mice

It should be noted, again, that these results are constants determined at the steady state, while in general, the reproduction and differentiation rates are functions of cell population and time. It is also important to note that these scientists also simplified the life span of the stem cells to one G_0 cycle. Hence their parameters values correspond to the values in this paper and are indeed relevant.

For the normal stem cell population, we will use the averages of the estimates for the apoptosis rate (a), the differentiation rate (δ), and the delay time (t_0) of 0.10, 0.025, and 2.83 days. Next, in finding our parameter β, we wish to ensure that our choice keeps the model consistent in the sense that these parameters will allow a steady state to exist. Referring back to 3.18, we need $R(S^*) = D(S^*)$, which requires

$$2(1-a)S^*\beta(S^*) = S^*(\beta(S^*) + \delta). \tag{4.1}$$

This leads to our steady state value for the reproduction parameter,

$$\beta(S^*) = \frac{\delta}{1-2a} = \frac{0.025}{1-2*0.1} \approx 0.031\ day^{-1}, \tag{4.2}$$

which, reassuringly, fits very nicely into the range from table 4.1. We use the same value for the time scale of normal stem cell growth, $\lambda_s = 0.2\ days^{-1}$, as that used by Murray [29] to simulate a model by Mackey and Glass for hematopoiesis. The use of the λ term in their model is very similar to that in ours and hence, this seems reasonable.

Hence, If we calculate the nondimensional parameter values and insert them into our nondimensional equation for the single population 3.19, we get

$$\dot{S} = 1.8\frac{S(t-0.566)}{1+S(t-0.566)^2} - \frac{S}{1+S^2} - 0.125S. \tag{4.3}$$

The dimensional parameter values we use for the single population model are listed in table 4.2.

$a\ (day^{-1})$	$\lambda_s\ (day^{-1})$	$\delta_s\ (day^{-1})$	$t_0\ days$
0.01	0.2	0.025	2.83

Table 4.2: Parameter Values for Single Population Model

4.2 Numerical Solution for Single Population

Equation 4.3 is a delay differential equation and could not be solved numerically using only the standard MATLAB functions. I was able to solve the equation using a MATLAB program and documentation posted on the world-wide-web by Lawrence F. Shampine and S. Thompson [34] [33]. Using four of these programs (dde23.m, ddeget.m, ddeset.m, ddeval.m), I coded a short file to solve 4.3 numerically[1]. The delay parameter must be nondimensionalized using our time scale λ_s and hence is inputted into the program as 0.566 (0.566=2.83×0.2). Figure 4.1 shows how, for the parameter values listed in table 4.2, the stem cells will proliferate from a very small, though non-zero, initial population to a steady state in roughly 150 days, which seems reasonable. This value, though, changes to some extent if one alters the size of the initial population.

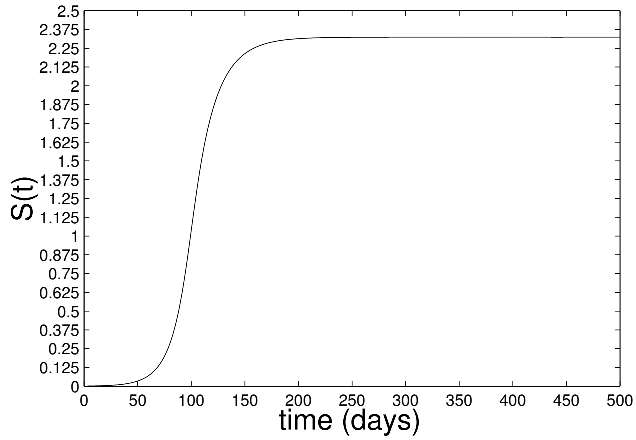

Figure 4.1: Trajectory of Stem Cell Population with Delay of 2.83 Days and Parameters as in Table 4.2

When we determined the linear stability of this steady state, we found that there would be a bifurcation to oscillatory instability as the value of μ dropped below the level of the bifurcation line in figure 3.10. Given our parameter values, we can calculate μ and ν as follows

$$\mu = \tau R'(S^*) = \tau(\frac{2(1-a)}{1+S^{*2}} - \frac{4(1-a)S^{*2}}{(1+S^{*2})^2}) = 0.566(-0.1934) = -0.11, \qquad (4.4)$$

and

$$\nu = \tau D'(S^*) = \tau(\frac{1}{1+S^{*2}} - \frac{2S^{*2}}{(1+(S^{*2})^2} + q) = 0.566(0.0176) = 0.01. \qquad (4.5)$$

For this small value of ν, μ must be less than approximately -1.60 to bifurcate to instability. Clearly, these parameters put the single population steady state within a

[1]See Appendix B for code.

stable range as $-0.11 > -1.60$. This stability is confirmed by the plot in figure 4.2 of equation 4.3 with the starting value set slightly higher (a small perturbation) than the steady state. Clearly, the amount of cells returns from the perturbed value to the steady state.

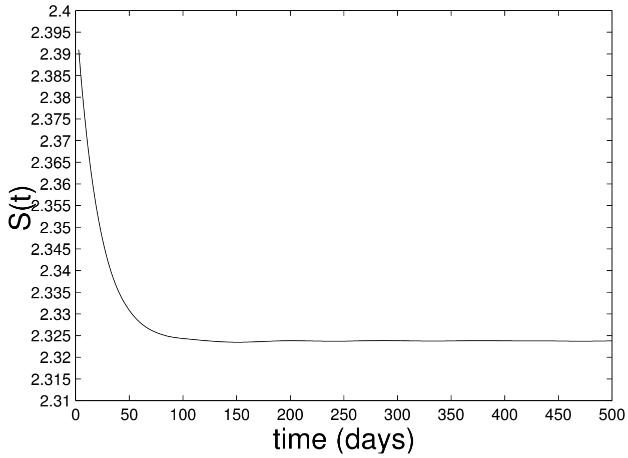

Figure 4.2: Perturbation from Steady State with Delay of 2.83 Days and Parameters as in Table 4.2

Now we would like to test our model by considering what happens as the delay increases, thus decreasing μ toward the bifurcation value. Increasing the delay, t_0, will increase both ν and $|\mu|$. I ran the single population model with increasing values of t_0 and found oscillatory instability when I reached the critical delay of 43.75 days.

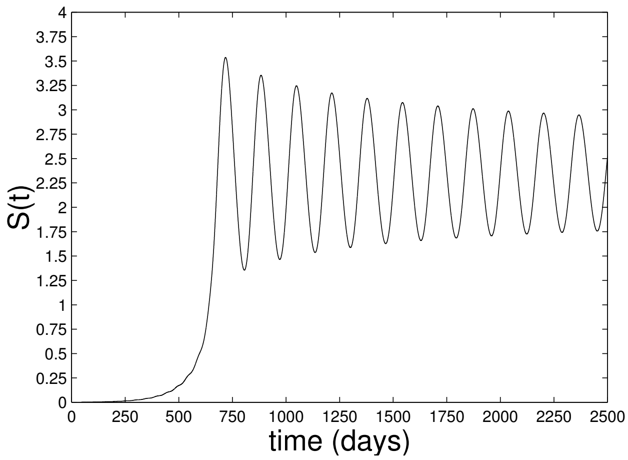

Figure 4.3: Trajectory of Stem Cell Population with Delay of 43.75 Days and Other Parameters as in Table 4.2

Indeed, this delay gave rise to oscillations when the stem cells began from a near zero population. When the cell population began from a slight bifurcation from the steady state, the oscillations increased in amplitude. One can clearly see this instability in these two respective plots with the delay of 43.75 days, shown in figures 4.3 and 4.4.

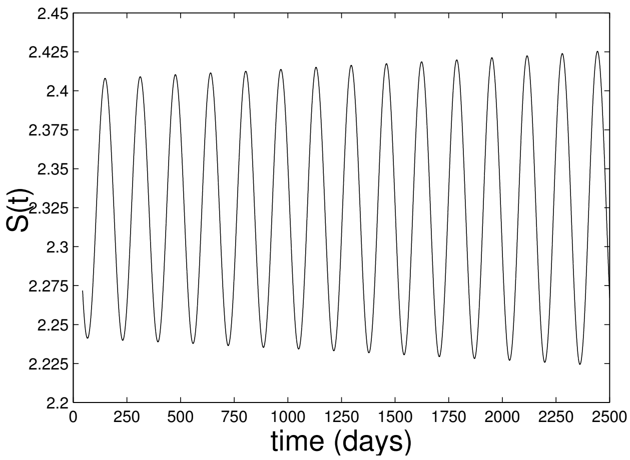

Figure 4.4: Perturbation from Steady State with Delay of 43.75 Days and Other Parameters as in Table 4.2

With a delay of 43.75 days, we recalculate $\mu = (43.75 * 0.2)(-0.1934) = -1.69$, and $\nu = (43.75 * 0.2)(0.0176) = 0.15$. Referring to figure 3.10, the ν, μ coordinate of (0.15,-1.69) lies just below the bifurcation line. Indeed, our numerical simulation has verified the results from our earlier linear stability analysis.

4.3 Numerical Solution for System of Normal and Abnormal Cells

Now, we will numerically solve the system of equations given in 3.40 and 3.41. We already have the parameters $\lambda_s = 0.2\ days^{-1}$, $\delta_s = 0.025$, $a = 0.1$, but need to find values for the abnormal cells' apoptosis rate (b), time scale (λ_a), niche or compression advantage (g), and differentiation rate (δ_a). We know from our logistic growth model that $g > 1$ to reasonably reflect the abnormal cells' growth advantage. Hence, we will choose $g = 2$. Also, as discussed in chapters 1 and 2, when the abnormal cell population reaches late stages, many of the cells do not differentiate properly, if at all. Our model does not have an age-dependency and hence, we will attempt to inject this characteristic into the model by making the differentiation rate half that of the normal cells. This is a reasonably significant difference, though leaves the differentiation rate far greater than zero at $\delta_a = 0.0125$. Clinical data has also shown that the apoptosis rate in CML patients is lower than that in healthy patients [27]. Hence, we will set

$b = 0.05$, or half of the normal apoptosis rate. For now, we will leave the time scale for the abnormal cells the same as those of normal cells and will numerically solve from a state where the normal population is very close to equilibrium but a tiny population of abnormal cells (again, 0.001) exists. The dimensional parameter values that are used for the abnormal cell population are listed in table 4.3.

b (day^{-1})	λ_a (day^{-1})	δ_a (day^{-1})	t_0 $days$
0.005	0.2	0.0125	2.83

Table 4.3: Parameter Values for Abnormal Stem Cell Population

To solve the system numerically, I have again written a code[2] which uses the four programs written by Shampine and Thompson [34]. The plot in figure 4.5 shows that, with the parameters in tables 4.2 and 4.3, the abnormal population will proliferate to a positive steady state in roughly two years. The population of normal cells will remain close to the steady state plateau for about 6 months and then decline rapidly until it is eliminated completely. This proves consistent with equation 3.51 which says that, with these parameters, there should be no steady states with positive values for both normal and abnormal cells.

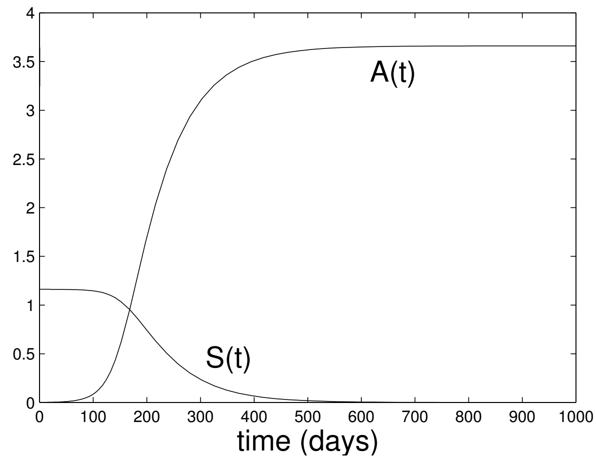

Figure 4.5: Trajectories of Normal and Abnormal Populations with Delay of 2.83 Days and Other Parameters as in Tables 4.2 and 4.3.

Altering the parameter value for the time scale of the abnormal cells, we may obtain a significantly slower or more rapid convergence to these equilibrium values. However, as long as the parameters do not satisfy inequality 3.51 and there is a positive population of abnormal cells, the normal cell population will be eliminated.

[2]See Appendix B for code.

We would now like to examine the stability of the steady state with $S = 0$ and $A = A^*$. We know that the same bifurcation relationship holds between μ_3 and ν_3 as defined in equations 3.74 and 3.75 as that which held for the single population between μ and ν. This parameter space is relevant for a perturbation of both the S and A populations as our definitions of μ_3 and ν_3 hold when $C \neq 0$ in equation 3.70. We can calculate μ_3 and ν_3 as follows

$$\mu_3 = \tau \frac{dR_1}{dS}(0, A^*) = \tau(\frac{2(1-a)}{1+A^{*2}}) = 0.566(0.1250) = 0.07, \tag{4.6}$$

and

$$\nu_3 = \tau \frac{dD_1}{dS}(0, A^*) = \tau(\frac{1}{1+A^{*2}} + q_s) = 0.566(0.1949) = 0.11. \tag{4.7}$$

From the plot in figure 3.10, we know that with positive ν_3, for there to be a bifurcation to oscillatory instability, μ_3 would have to be negative. It is clear that there is no positive value for the delay parameter, τ, which would lead to this type of bifurcation. Alternatively, we look for a bifurcation to a drift instability. This instability will arise when $\mu > \nu$. As such, it is clear that with these parameters, there is no way for a positive delay to lead to instability in both populations at the steady state of $S = 0$ and $A = A^*$.

We must now check, though, for the conditions leading to an instability only in the population of abnormal cells. This corresponds to the case where $C = 0$ and the relevant parameters are μ_4 and ν_4. We calculate that

$$\mu_4 = \tau \frac{dR_2}{dA}(0, A^*) = \tau(\frac{2(1-b)\rho}{1+A^{*2}} - \frac{4(1-b)\rho A^{*2}}{(1+A^{*2})^2}) = 0.566(-0.1136) = -0.06, \tag{4.8}$$

and

$$\nu_4 = \tau \frac{dD_2}{dA}(0, A^*) = \tau(\frac{\rho}{1+A^{*2}} - \frac{2\rho A^{*2}}{(1+A^{*2})^2} + q_a) = 0.566(-0.0027) = 0.00. \tag{4.9}$$

Hence, if we were to increase the delay sufficiently in this case, we would see oscillatory instability from this steady state when $\mu \approx -1.60$. Hence, when the delay equals $5\frac{1.60}{0.1136} = 70.5$ days, we should see oscillatory instability.

The MATLAB simulation in figure 4.6, run with the delay parameter just beyond this bifurcation point (72 days), shows the oscillatory instability that can arise from the steady state of all abnormal cells.

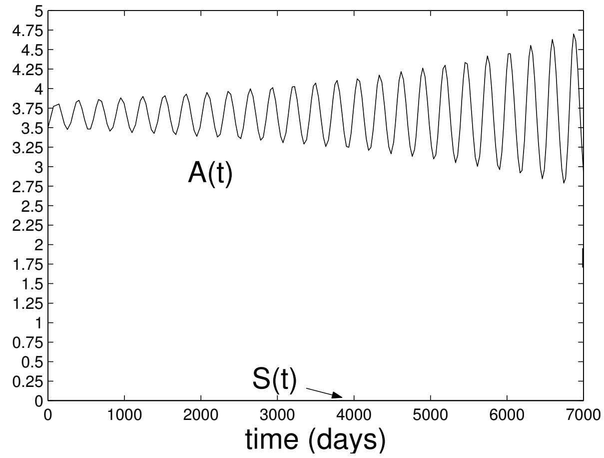

Figure 4.6: Oscillatory Instability from Steady State with $A = A^*$ and $S = 0$ with Delay of 72 Days and Other Parameters as in Tables 4.2 and 4.3

4.4 Possibility of Different Delays

In this section, we consider the possibility that the abnormal stems cells take longer to self-replicate. Some biologists feel that this delay term is presumably larger than that in the normal cells and this, in part, may lead to the instability [4]. Under this assumption, our system of nondimensional equations becomes

$$\dot{S} = 2(1-a)\frac{S(t-\tau_1)}{1+(gS(t-\tau_1)+A(t-\tau_1))^2} - \frac{S}{1+(gS+A)^2} - q_s S, \tag{4.10}$$

and

$$\dot{A} = 2(1-b)\rho\frac{A(t-\tau_2)}{1+(gS(t-\tau_2)+A(t-\tau_2))^2} - \frac{A}{1+(gS+A)^2} - q_a A, \tag{4.11}$$

where $\tau_1 < \tau_2$. With only a minor modification of program twopop.m[3], I plotted the trajectories of the normal cell count and the abnormal cell count from an initial steady state of $S = S^*$ and $A = 0$. When I solved the equation for $\tau_1 = 0.566$ (which lead to stability in the normal population) and $\tau_2 = 14.4$ (which lead to instability), the population quickly moves to the steady state of all abnormal cells and then oscillates with increasing amplitudes. Though the instability resembles clinical observations in CML, this numerical solution gives no indication of a chronic phase. This is shown in figure 4.7.

[3]See Appendix B for code.

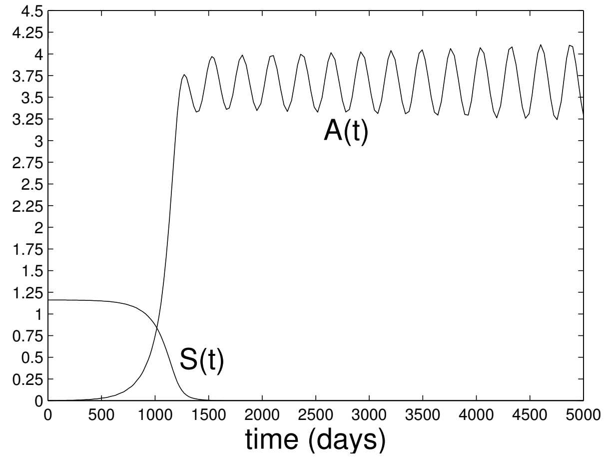

Figure 4.7: This figure shows the trajectories of the stem cell counts with different delays. The normal population has a delay of 2.83 days, and the abnormal stem cell population has a delay of 72 days. All other variables are as listed in tables 4.2 and 4.3.

We note, however, the possibility that the delay in the abnormal cells is the slowly moving variable we have been looking for. It seems plausible, though not probable, that numerous further mutations of the original abnormal cells would produce larger and larger delays. If this steady state is reached when the abnormal cells have a small enough delay, stability will be maintained. As the maximum delay in the abnormal population slowly increases toward the bifurcation value, this stability will be preserved. However, once enough mutations have ocurred to give some of the abnormal cells a large enough reproductive delay, the state will become unstable as it did in figure 4.7.

It should also be noted that the unstable delay used for the abnormal cells is on the order of 70 days, a ridiculously large amount of time for a cell to reproduce itself. Hence, this scenario should simply be viewed as an interesting way in which the cell counts' trajectories might be influenced by differing delay factors.

4.5 Third Non-Trivial Steady State

In this section, we return to our assumption that there is only one delay parameter, and we try to simulate what happens if the parameters are such that there is a steady state with positive normal and abnormal cell populations. In subsection 3.5.2, we made a comparison of this model to the less complex logistic model and predicted that if this steady state exists, it will be stable. Leaving all the other parameters as shown in tables 4.2 and 4.3, we let $\rho = 0.5$ and $q_a = 0.1$. This gives us a steady state with both positive normal and abnormal cells. We now refer back to section 3.5.2. We determined that for stability, the real portion of σ must be less than or equal to zero where

$$\sigma^2 - \sigma Tr(\mathcal{J}) + Det(\mathcal{J}) = 0. \tag{4.12}$$

Using our parameter values and substituting into equation 3.83 for the Jacobian $\mathcal{J}$, we find that

$$\mathcal{J} = \begin{pmatrix} 0.0962e^{-\sigma\tau} - 0.1784 & -0.0925e^{-\sigma\tau} + 0.0514 \\ -0.2489e^{-\sigma\tau} + 0.1310 & -0.0378e^{-\sigma\tau} - 0.0801 \end{pmatrix}. \tag{4.13}$$

The stability characteristics for equations of the form of 4.12 are shown in the diagram in figure 4.8. We clearly see that for stability, we need the trace of $\mathcal{J}$ to be negative, and the determinant of $\mathcal{J}$ to be positive. Once either of these conditions fails to be true, the steady state will become unstable.

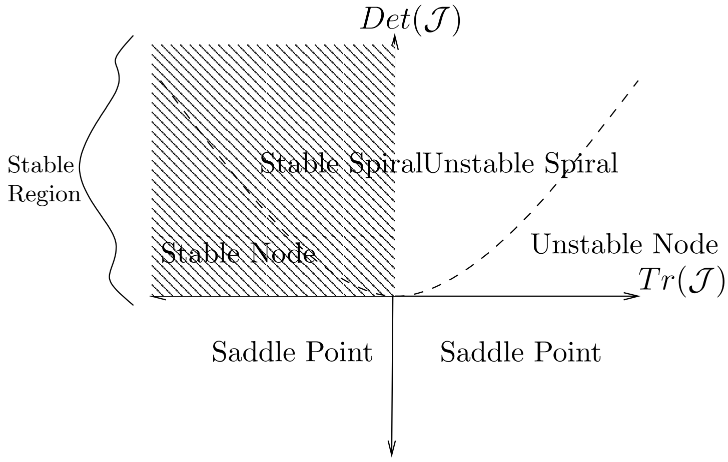

Figure 4.8: Stability Regions for Characteristic Polynomial

Hence, if we start by assuming that there is no delay ($\tau = 0$), then

$$Tr(\mathcal{J}) = 0.0584e^{-\sigma\tau} - 0.2585 = 0.0584 - 0.2585 < 0, \tag{4.14}$$

and

$$Det(\mathcal{J}) = -0.0266e^{-2\sigma\tau} + 0.0239e^{-\sigma\tau} + 0.0076 = -0.0266 + 0.0239 + 0.0076 > 0. \tag{4.15}$$

These values for the trace and determinant of $\mathcal{J}$ put the system in the second quadrant of figure 4.8, indicating that without a delay, the steady state is stable.

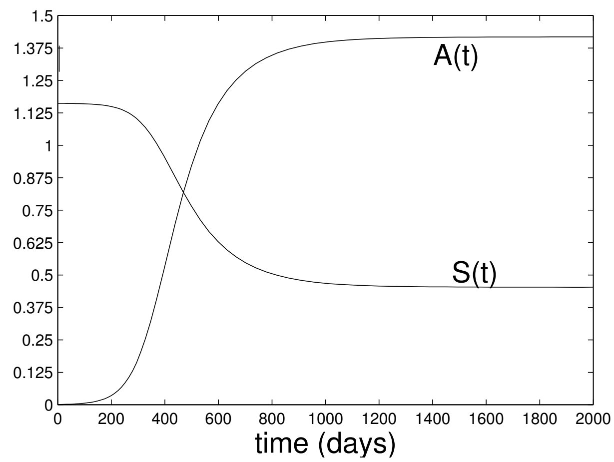

Figure 4.9: Stability of the third steady state with no delay, $\rho_a = 0.5$, $q_a = 0.10$, and other parameters as listed in tables 4.2 and 4.3.

This is verified by the convergence of the two populations to these steady states from the population of all normal cells in figure 4.9. Our assumption of stability, based on comparisons with the logistic model, was indeed correct.

The problem with using this framework to determine if a critical delay exists, is that if $\tau > 0$, then both the determinant and the trace of $\mathcal{J}$ contain an exponential term in $\sigma\tau$ and the diagram in figure 4.8 no longer holds. Thus, solving analytically for the critical delay can be quite complex and will not be further pursued.[4] Numerically, I tested for a delay which might lead to oscillatory instability in both populations from their positive steady states. I found that a critical delay of about 76 days does exist.

[4]An approach to a nearly identical problem can be found in Tam [35].

Chapter 5

Addition of the Immune Response

5.1 Mathematical Model

Dealing only with the dynamics of hematopoietic stem cell production and maturation, we gained a lot of insight into how the disease progresses. At this point, we do not know how the immune response will affect CML, if at all. Hence, we aim to add the basic facets of the immune response into our model. Referring back to sections 3.2 and 3.5 in chapter 3, we inject the impact of the immune system in equations 3.1 and 3.2 into the G_0 model equations, 3.40 and 3.41. We also consider, as we did in section 4.4 the possibility that the abnormal cells have a different reproduction time than the normal stem cells. This gives us a far more complex model for the normal and abnormal cell populations:

$$\dot{S} = 2(1-a)\frac{S_{t_s}\lambda_s}{1+(\frac{gS_{t_s}+A_{t_s}}{A_p})^2} - \frac{S\lambda_s}{1+(\frac{gS+A}{A_p})^2} - S\delta_s \tag{5.1}$$

and

$$\dot{A} = 2(1-b)\frac{A_{t_a}\lambda_a}{1+(\frac{S_{t_a}+A_{t_a}}{A_p})^2} - \frac{A\lambda_a}{1+(\frac{S+A}{A_p})^2} - A\delta_a - \beta_{ta}TA, \tag{5.2}$$

where the additional decay term represents the elimination of abnormal cells by the activated T cells. In accordance with the law of mass action, this occurs at a rate proportional to the product of the T cell and the abnormal stem cell populations. We have called the proportionality constant β_{ta} and will also use this labeling practice for the proportionality constants of the other mass action rates.

The population of normal dendrites satisfies

$$\dot{D} = \lambda_d S(t-t_d) - \mu_d D - \beta_{da} D A_d, \tag{5.3}$$

where the growth term represents the stem cells differentiating with a delay to form mature dendrite cells. The decay terms represent the death rate and the amount of dendrites which, at a speed governed by the law of mass action, consume dead abnormal stem cells. After consuming the dead abnormal cells, they express abnormal proteins and join the population denoted by C.

Abnormal dendrites, X, have the same growth and decay terms except they do not have the ability to join class C because abnormal dendrites will not recognize abnormal stem cells as being a target for the immune system. Hence, abnormal dendrites will not activate T cells even after consuming dead abnormal stem cells. Thus, we have

$$\dot{X} = \lambda_x A(t - t_x) - \mu_x X. \tag{5.4}$$

The equation for the population of dead abnormal stem cells, A_d, involves the natural death of the abnormal cells, their death via immune response, and their consumption by the dendrites. Hence,

$$\dot{A}_d = q_{ad} A + \beta_{ta} T A - \beta_{da} D A_d. \tag{5.5}$$

As the above loss term represents the ingestion of dead abnormal cells by normal dendrites, this is a birth term for the population of dendrites expressing abnormal proteins, C. Thus, we have

$$\dot{C} = \beta_{da} D A_d - \mu_d C, \tag{5.6}$$

where μ_d is the still the death rate of normal dendrites, whether they express abnormal proteins or not.

Finally, we must introduce equations for the two types of T cells in our system: resting (R) and active (T). Some proportion of the initial population of resting T cells, R_0, are first activated when they encounter dendrites which express abnormal proteins, C. Once active, though, they return to the resting state upon encountering an abnormal dendrite as the abnormal dendrite will not express any abnormal proteins. Hence, the resting cells satisfy

$$\dot{R} = \beta_{xt} X T - \beta_{rc} R f(C). \tag{5.7}$$

The decay factor above involves a function f because the immune system should activate T cells very rapidly above some threshold for the amount of dendrites expressing abnormal proteins, while it should not activate resting T cells when the count is very low. The count of active T cells is increased by activation of resting cells and by signals sent from other already active T cells which encounter dendrites expressing abnormal proteins. These cells return to the resting phase upon encountering abnormal dendrites or normal dendrites that are not expressing abnormal proteins. Thus,

$$\dot{T} = \beta_{ct}CT + \beta_{rc}Rf(C) - \beta_{xt}(X + D)T. \tag{5.8}$$

5.1.1 Activation of Resting Cells

We first consider the shape of the function determining the rate of activation of resting T cells in response to dendrites expressing abnormal proteins. The function should only be a function of C, and across a non-negative domain, the function's range should also be non-negative. Again, we would like the function to be such that below some threshold, the rate remains very small or zero, while above the threshold, the rate increases linearly. As such, we simply choose

$$f(C) = (C - C_p)_+, \tag{5.9}$$

where C_p is this threshold.

5.1.2 Nondimensionalization

Once again, the first step to our analysis of the model will be to nondimensionalize the equations. In choosing concentration scales for these various entities, one must be aware of some fundamental differences between the biological entities composing the immune response and the actual hematopoietic stem cells. While the agents of the immune system are in the peripheral blood, only a portion of the stem cells are in the actual blood stream. A large portion of the stem cells are in the bone marrow itself. If one envisions the dendrites and T cells passing over the marrow, then their interaction and measure of concentration will differ from the case when they are evenly distributed throughout the blood stream. Most data on stem cell counts, though, has been measured in cells per liter of peripheral blood. Therefore, we will consider the later case where the entire system is evenly distributed in the blood stream. This assumption also is allows us to model the interaction with the immune system according to the law of mass action.

We use similar nomenclature as before for the nondimensional variables and parameters and use the same time and concentration scales[1]. For ease of notation, the following table lists the scales used for nondimensionalization of each dimensional variable.

Dimensional Variables or Parameters	Scale Used
$S,\ A,\ D,\ X,\ A_d,\ C,\ R,\ T$	A_p
$t,\ t_s,\ t_a,\ t_d,\ t_x$	$\frac{1}{\lambda_s}$

We also will define the following nondimensional variables:

$$
\begin{aligned}
\rho_a &= \frac{\lambda_a}{\lambda_s},\ \rho_d = \frac{\lambda_d}{\lambda_s},\ \rho_x = \frac{\lambda_x}{\lambda_s}, q_s = \frac{\delta_s}{\lambda_s},\ q_a = \frac{\delta_a}{\lambda_s},\ q_d = \frac{\mu_d}{\lambda_s},\ q_x = \frac{\mu_x}{\lambda_s},\ q_{ad} = \frac{\mu_{ad}}{\lambda_s},\ q_c = \frac{\mu_c}{\lambda_s}, \\
\kappa_{ta} &= \frac{A_p\beta_{ta}}{\lambda_s},\ \kappa_{da} = \frac{A_p\beta_{da}}{\lambda_s},\ \kappa_{xt} = \frac{A_p\beta_{xt}}{\lambda_s},\ \kappa_{rc} = \frac{A_p\beta_{rc}}{\lambda_s},\ \kappa_{ct} = \frac{A_p\beta_{ct}}{\lambda_s},\ C_0 = \frac{C_p}{A_p}. \qquad (5.10)
\end{aligned}
$$

Using these nondimensional variables and parameters, we write the nondimensional mathematical model,

$$
\begin{aligned}
\dot{S} &= 2(1-a)\frac{S_{\tau_s}}{1+(gS_{\tau_s}+A_{\tau_s})^2} - \frac{S}{1+(gS+A)^2} - q_s S, && (5.11)\\
\dot{A} &= 2(1-b)\frac{\rho_a A_{\tau_a}}{1+(S_{\tau_a}+A_{\tau_a})^2} - \frac{\rho_a A}{1+(S+A)^2} - q_a A - \kappa_{ta} TA, && (5.12)\\
\dot{D} &= \rho_d S_{\tau_d} - q_d D - \kappa_{da} D A_d, && (5.13)\\
\dot{X} &= \rho_x A_{\tau_x} - q_x X, && (5.14)\\
\dot{A}_d &= q_{ad} A + \kappa_{ta} TA - \kappa_{da} D A_d, && (5.15)\\
\dot{C} &= \kappa_{da} D A_d - q_d C, && (5.16)\\
\dot{R} &= \kappa_{xt} XT - \kappa_{rc} R (C - C_0)_+, && (5.17)\\
\dot{T} &= \kappa_{ct} CT + \kappa_{rc}\chi R(C-C_0)_+ - \kappa_{xt}(X+D)T. && (5.18)
\end{aligned}
$$

5.1.3 Initial Conditions

Initially, we assume that there is only one abnormal stem cell in the entire body and that it is alive. Hence, there will have been no dendritic activation of T cells. Thus, at $t = 0$,

$$T = C = X = A_d = 0, \qquad (5.19)$$

[1]For instance, $\tau_s = t_s\lambda_s$, etc.

and a reasonable choice for our initial dendrite population is its disease-free steady state,

$$D_0 = \frac{\rho_d S_0^b}{q_d}. \tag{5.20}$$

5.1.4 Preliminary Qualitative Analysis

Unlike the previous models, this model is eight dimensional and it is not trivial to search for a steady state analytically. Hence, before we attempt to do so, we want to think about how the model works and have a general understanding of its dynamics. To start, we notice that the only difference in the equations for S and A is the addition of the $\kappa_{ta}AT$ term. In particular, we note the fact that the $\kappa_{ta}T$ term augments the differentiation and death rate, q_a. Given that T will change over time, we should consider the possibility that this addition represents a slow drift through parameter space over time.

Further, we know that the population of normal cells gives rise to normal dendrites, after some time delay. When abnormal cells exist, they will slowly die. Normal dendrites will ultimately consume these dead cells and this will trigger the activation of resting T cells into active T cells. Hence, it is the combination of abnormal dead cells and the production of normal dendrites from normal stem cells which will trigger the immune systems' killing of the abnormal cells. Because the immune response is proportional to the amount of dead abnormal cells, this is, in effect, a positive feedback loop. However, we see that abnormal cells give rise to abnormal dendrites which shut down the immune response. Hence, we see that for an immune response to continue, there must be some population of normal stem cells (as they provide normal dendrites). Once these cells are killed, the population of normal dendrites will vanish, and nothing will exist to activate the resting T cells.

Given the slow progression of the chronic phase into the rapidly changing acute phase, we consider the idea that our system involves fast and slow variables. Given that the immune system is designed to react in a matter of days, weeks, or months, while the chronic phase of CML lasts years, we will assume the immune response is rapid compared to the proliferation of the abnormal stem cells. This assumption will guide the analysis in this chapter.

It is also apparent that the key component of the system of stem cells is A, the abnormal stem cell population, while that of the immune response is T, the active T cell count. We will seek to represent the fundamental dynamics of this complex eight-dimensional system with the interaction between the two key populations, A and T.

First, we will consider if a relatively quick immune response can have a quasi-steady state. If we find such a quasi-steady state, we will look for a slow moving variable that might cause the system to slowly drift along an equilibrium surface. Perhaps if this equilibrium surface has a nonmonotonic dependence on A, then the drift could cause the system to "fall off" the equilibrium surface.

5.1.5 Quasi-Steady State

R, the amount of resting T cells, is relevant in our model as a precursor to T, the active T cells. We start with the assumption that the amount of resting T cells, R, is extremely large compared with the rest of the entities in the system. This assumption allows us to consider R at a near-steady state if κ_{rc} is small, because then the terms in equation 5.17 for $\dot{R}$ will be relatively tiny compared to R_0. This assumption seems valid from a biological standpoint as the body, in a healthy state, presumably has an extremely large reserve of resting T cells.

Next, we consider a rapid immune response and solve for the steady state values. Setting equation 5.14 equal to zero, we find the steady state of the abnormal dendrites, X,

$$X = \frac{\rho_x}{q_x} A. \tag{5.21}$$

We do the same for the dendrites expressing abnormal proteins and see that

$$C = \frac{\kappa_{da} D A_d}{q_d}. \tag{5.22}$$

Noting the term $\kappa_{da} D A_d$ in equations 5.13 and 5.15 for the normal dendrites and dead abnormal cells, respectively, we can also express C in terms of the steady states of S and D, or of A and T. These expressions are,

$$C = \frac{\rho_d}{q_d} S - D = \left(\frac{q_{ad}}{q_d} + \frac{\kappa_{ta}}{q_d} T\right) A. \tag{5.23}$$

Solving for the steady state of T, the active T cell population, we find

$$T = \frac{\kappa_{rc} R (C - C_0)_+}{\kappa_{xt}(X + D) - \kappa_{ct} C}. \tag{5.24}$$

Using the expressions in equations 5.21 and 5.23 for X and D, respectively, we express T as follows,

$$T = \frac{\kappa_{rc} R (C - C_0)_+}{\dfrac{\kappa_{xt}\rho_x}{q_x} A + \dfrac{\kappa_{xt}\rho_d}{q_d} S - (\kappa_{xt} + \kappa_{ct}) C}. \tag{5.25}$$

As we would like to focus on A, we suppose, for example, that $\frac{\kappa_{xt}\rho_d}{q_d} S \ll 1$. With that condition, equations 5.23 and 5.25 form a system of two equations in the variables T, C, and A. We start with equation 5.23 and draw a rough sketch of how it would appear in C,T space for various values of A. This sketch is shown in figure 5.1.

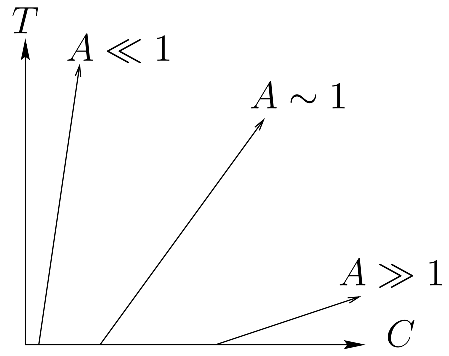

Figure 5.1: This sketch demonstrates the relationship between the active T cells, the dendrites expressing abnormal proteins, and the abnormal stem cells at equilibrium, as dictated by equation 5.23.

Provided that $\frac{\kappa_{xt}\rho_d}{q_d} S \ll 1$, equation 5.25 can be broken up as the product of the immune triggering function, $f(C)$, and a function of the form $\frac{b_1}{b_2 A - b_3 C}$, where b_1, b_2, and b_3 are constants. We consider this product graphically. Figure 5.2 shows the basic shape of $f(C)$ and $\frac{b_1}{b_2 A - b_3 C}$ in C,T space. Figure 5.3 then shows the product of these functions, for different values of A.

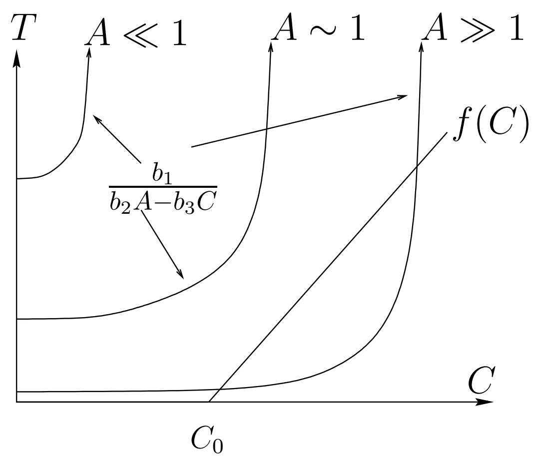

Figure 5.2: Factoring the equation for T into the functions $f(C)$ and $\frac{b_1}{b_2 A - b_3 C}$.

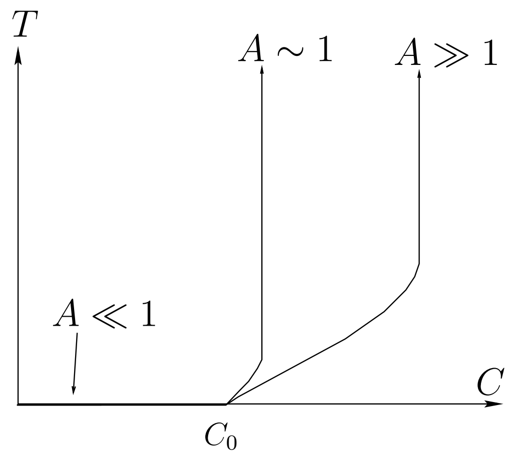

Figure 5.3: This sketch demonstrates the relationship between the active T cells, the dendrites expressing abnormal proteins, and the abnormal stem cells at equilibrium, as dictated by equation 5.25.

Finally, we now consider where the curves in figure 5.1 and figure 5.3 intersect. These intersections, shown in figure 5.4 should represent coordinates for T, C, and A at a quasi-equilibrium.

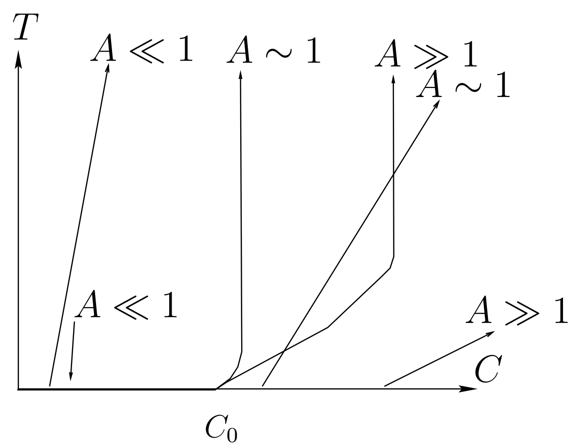

Figure 5.4: Intersections in T, C, A Space Indicating Quasi-Equilibrium Values

We see in figure 5.4 that depending on the parameters, we may have from zero to two intersections for a given value of A. This implies that over a certain range, each value of A corresponds with two equilibrium values for T. Essentially, this means that the equilibrium manifold, or nullcline, for T as a function of A folds back on itself as shown in figure 5.5.

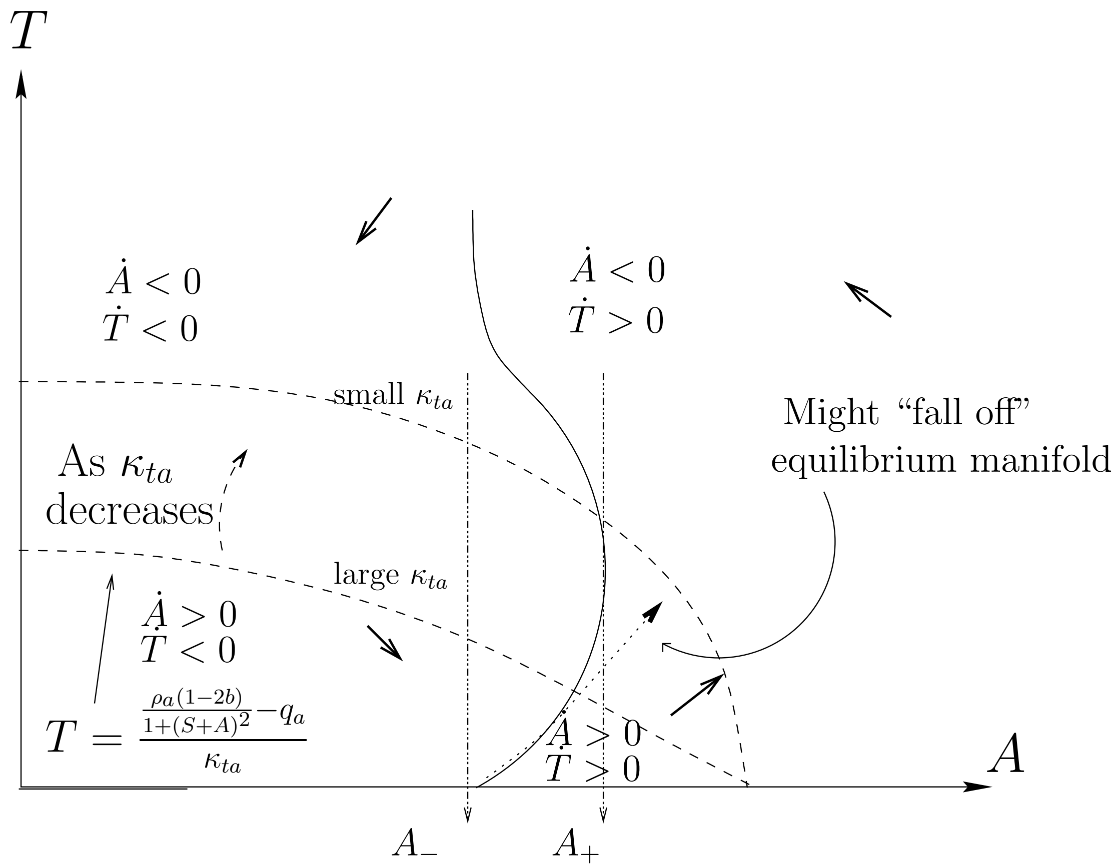

Figure 5.5: One can see that the equilibrium curve bends back onto itself. As κ_{ta} decreases the equilibrium involves greater amounts of active T cells. It is plausible that rather than bend back onto itself, the abnormal cell count continues to increase and "falls off" the equilibrium curve.

Conditions for A to lie on Curved Section of Equilibrium Manifold

One notes in figure 5.5 that there is a strict range through which A must pass for this scenario to be possible. If $A \notin (A_-, A_+)$, then the equilibrium value will not be along the part of the curve which bends onto itself. The value for A_- is simply the minimum value of A necessary for the curves in figure 5.3 to have a positive value. If A is too small, the curves will have asymptotes at C values less than C_0 and hence, will be multiplied by zero over their entire domain. A will reach this critical point when the asymptote dictated by the denominator in equation 5.25 is located at $C = C_0$. Again, assuming that $\frac{\kappa_{xt}\rho_d}{q_d} S \ll 1$, we set the denominator of equation 5.25 equal to zero at $C = C_0$ and find,

$$A_- = C_0 \frac{q_x(\kappa_{xt} + \kappa_{ct})}{\rho_x \kappa_{xt}}. \tag{5.26}$$

Conversely, if A is so large that equation 5.23 crosses the C axis in figure 5.1 at a point greater than C_0, there might not be an intersection in the graph in figure 5.4 and hence, there might not be an equilibrium.[2] Setting $T = 0$ in equation 5.23, we see that for the curve to cross the C axis at C_0, $A = \frac{C_0 q_d}{q_{ad}}$. Hence,

$$A_+ \geq C_0 \frac{q_d}{q_{ad}}, \tag{5.27}$$

and putting these inequalities together, we find that for our hypothesis to be at all possible, the system would have to be such that

$$C_0 \frac{q_x(\kappa_{xt} + \kappa_{ct})}{\rho_x \kappa_{xt}} < A < C_0 \frac{q_d}{q_{ad}}. \tag{5.28}$$

Simplifying equation 5.28, we derive the fundamental condition which guarantees a multiplicity of steady states for some positive value of A:

$$\frac{q_x(\kappa_{xt} + \kappa_{ct})}{\rho_x \kappa_{xt}} < \frac{q_d}{q_{ad}}. \tag{5.29}$$

Next, we would like to sketch the basic shape of the nullclines for A as the intersection between these two nullclines determines the equilibrium position for the system. The nullcline for A is found by setting equation 5.12 equal to zero (and ignoring the delay terms). The equation for the nullcline is

$$T = \frac{\frac{\rho_a(1-2b)}{1+(S+A)^2} - q_a}{\kappa_{ta}}. \tag{5.30}$$

Maintaining our assumption that $A \gg S$, we ignore the S term when drawing the nullclines.

5.1.6 Slow Drifting Variable

One can now also draw arrows which indicate the trajectory the system should take based on the location relative to these nullclines. These arrows are included in figure 5.5. One possibility we would like to consider is that the system starts with a large κ_{ta} and is in an equilibrium position with a small active T cell count. As the disease wears the immune response down, there is a slow downward drift in the value of κ_{ta} which causes both the T cell count and the abnormal cell count to increase as they move along the T equilibrium curve. When the equilibrium curve bends back onto

[2]This is not necessarily the case as there may be a value for A such that the C intercept is greater than C_0 yet the slope is large enough that there are two intersections. The middle value of A in figure 5.4 demonstrates this possibility.

itself, there is the possibility that the abnormal population will not decrease rapidly enough to maintain its position on the equilibrium manifold. Hence, it could "fall off" and head toward a different steady state or become unstable.

Though it is logical to consider κ_{ta} to be the slowly drifting variable, it also seems promising to study the possibility that the resting T cell population, R, is the slowly moving variable. In the body there is a relatively large amount of resting T cells waiting to be activated. When the rest of the immune system is in equilibrium, the resting T cell population should slowly drift toward some steady state. We do not need to know what this steady state is to examine the effects of this drift.

To consider the effects of a slow drift in R, we refer back to the equation 5.25 and the sketch of its two factors, $f(C)$ and $\frac{b_1}{b_2A-b_3C}$, in figure 5.2. An increase in the value of R would not affect the function $f(C)$, but it would affect the curves, because $b_1 \sim R$. These curves would shift upward to higher T values for every value of C, though location of the asymptote would not change. When we multiply these new curves by the function $f(C)$, as in figure 5.3, the product still equals zero for $C < C_0$ and becomes asymptotic at the same value of C. In between these these two extremes, though, the new function is steeper than one with a smaller value of R. This is shown graphically in figure 5.6.

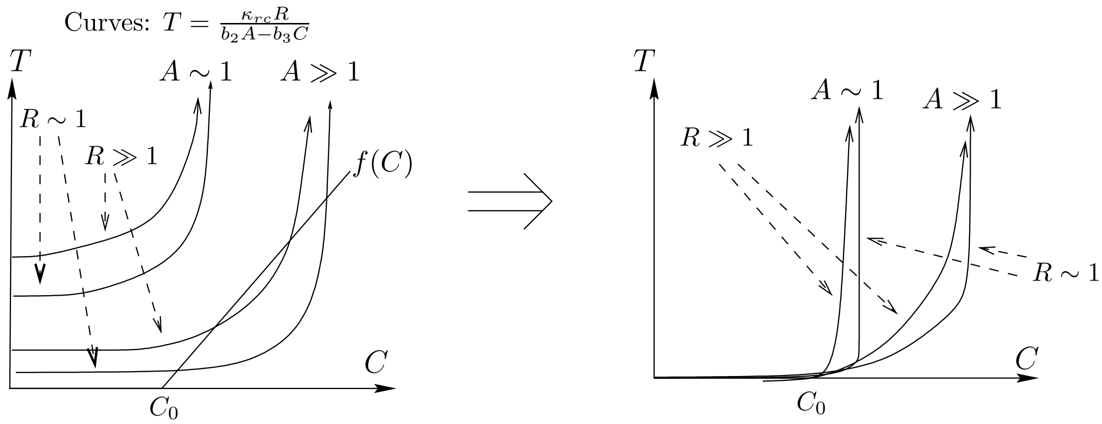

Figure 5.6: We can see the effect of an increase in the population of resting T cells, R, by considering the sketches of equation 5.25 in figures 5.2 and 5.3 for varying values of R. Functions with different values of R will still equal zero until they reach C_0 and will become asymptotes at the same C value. In between these two points, though, the curve will be steeper for greater R values.

The result of this increase in R is a shift to the left of the curved vertical nullcline in figure 5.5 in A,T space. This shift is not uniform, and the point where the nullcline intercepts the A axis, A_-, does not change with R. This shift, though, produces a similar effect to the upward shifting of the horizontal nullcline for points that are near, but on the bottom side, of the bend in the equilibrium manifold. If an equilibrium is reached when $A \in (A_-, A_+)$ and R begins to slowly increase, this drift will push this equilibrium closer to the peak of the manifold. Similar to the argument for a drift of κ_{ta}, this may push the equilibrium off of the manifold resulting in instability or convergence to a different steady state. This argument is illustrated in figure 5.7.

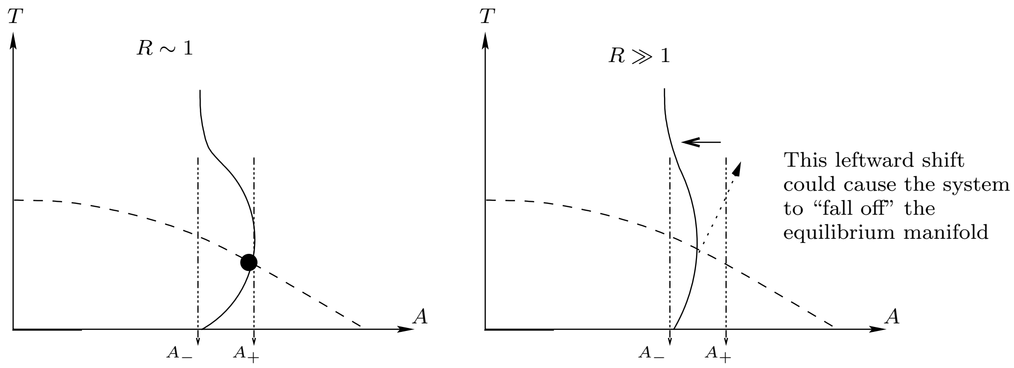

Figure 5.7: This figure shows how an increase in the number of resting T cells will result in a leftward shift of the vertical equilibrium manifold in A,T space. We see that an equilibrium below the curve's "nose" could be "pushed" off of the manifold by a sufficient increase in R.

5.2 Numerical Analysis

5.2.1 Parameter Values

It is extremely difficult to find data from which to extract parameter values for this model. Biologists are currently culturing cells and attempting to better measure these types of parameters, but the results of these studies might not be conclusive and will not be available very soon [4]. Hence, at this point, rather than concern ourselves with vague estimates of the parameters, we will choose them to illustrate the mechanisms we have mentioned.

One basic characteristic of the model is that if the normal stem cells become completely extinct, the normal dendrites will die out and ultimately, there will be absolutely no activation of the T cells. In CML cases, though the normal stem cell count does indeed steeply decrease, it does remains positive. Hence, we set the abnormal time scale parameter such that a steady state exists with positive levels of normal and abnormal cells. This steady state, though, still involves a relatively small amount of normal cells and a clear dominance of the abnormal population.

Next, we note that our hypothesis relies very heavily on the idea that the reaction of the immune system is rapid. Hence, the immune response must be on a very fast time scale compared with that of the normal and abnormal stem cells. As such, we have chosen the ratio of the time scales for the immune system to that of the normal stem cells, ρ_d and ρ_x, to be very large (they are both $\sim O(10)$). To try to slow the scale for the abnormal cells, we have reduced ρ_a to 0.5. We are unable to reduce the abnormal time scale much further as that would take the system out of the shaded region in the parameter space of figure 3.51, and the abnormal population would go to zero. For the nondimensional death rates (the q's) we have chosen parameter values from 0.1 to 0.2 as these rates are very close to those for the normal and abnormal stem cells. The nondimensional mass action constants (the κ's) were also all set between 0.1 and 0.2, except for κ_{rc} and κ_{ta}. κ_{rc} was set very low ($\sim O(10^{-4})$) because this constant was always multiplied by R, which had an extremely large starting value ($\sim O(10^5)$). The complete set of parameter values used is given in table 5.1.

$g = 2$	$q_s = 0.125$	$\rho_a = 0.5$	$\kappa_{da} = 0.1$
$a = 0.1$	$q_a = 0.100$	$\rho_d = 10$	$\kappa_{xt} = 0.2$
$b = 0.05$	$q_d = 0.1$	$\rho_x = 10$	$\kappa_{rc} = 0.001$
$C_0 = 0.1$	$q_x = 5$		$\kappa_{ct} = 0.15$

Table 5.1: Parameter Values Used for Numerical Simulation of Immune Response

The final nondimensional mass action constant, κ_{ta} was a primary focus of our numerical trials. This variable is singularly responsible in connecting the immune system to the stem cell populations and hence, we will set it to a variety of levels and witness the effect it has on the system. In particular, as mentioned earlier, our hypothesis is that a downward drift in its value might cause the abnormal population to "fall off" the equilibrium manifold.

Before we begin solving the equations, we would like to ensure that inequality 5.29 is satisfied and therefore, a bend in the vertical nullcline exists. Using the parameter values in table 5.1, we calculate that the inequality amounts to $0.875 < 10$ and hence, is indeed satisfied.

Lastly, we note that we will run the model without any time delays.

5.2.2 Immune Response Too Strong and Slow

Keeping the conditions as described above and using the parameters in table 5.1, the model was run with a very large κ_{ta} value of 10. The immune response that this prompted was either too slow, too strong, or was both. With these variables, the abnormal cells rose quickly toward a dominant steady state. Near their peak, though, a sharp impulse of active T cells arose and killed nearly all of the abnormal cells. When the abnormal cells were being killed, the normal cells grew toward dominance and the active T cell count subsided. This allowed the abnormal cell count to rise again, which then triggered a strong active T cell response, again, killing most of the abnormal population. This oscillatory pattern continued ad infinitum (or seemingly ad infinitum). The response of the active T cells as well as the amplitude of the abnormal cells' oscillations began to decay to a tiny extent which perhaps indicates that the system was moving toward some sort of equilibrium. This decay, however, was so minute, that the trajectories more closely resembled the periodic behavior associated with a limit cycle. Figure 5.8 shows the oscillations of the normal and abnormal cells with time and figure 5.9 illustrates the rapid impulse-like reactions of the active T cell population over time. Finally, it is important to note that with these parameters, violent oscillations emerged in the system even when κ_{ta} was reduced to order 1.

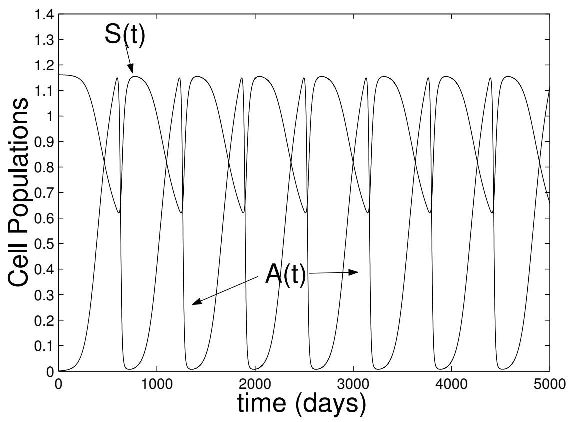

Figure 5.8: The extreme oscillations of the normal and abnormal stem cell populations in the case with $\kappa_{ta} = 10$ (other parameters the same as in table 5.1) are the result of an incredibly strong immune response. It is also possible, that the system is converging on an equilibrium, but that it is doing so at a remarkably slow rate. This would mean that the immune response is far too slow compared to the time scale of the abnormal cells.

We would also like to get a feel for the trajectory of this response in A,T space. One goal of these numerical simulations is to validate our assumption that the equilibria should resemble those sketched in figure 5.5. Though an equilibrium was not reached in this situation and hence, these trajectories through A,T space will presumably not follow the equilibrium curve of figure 5.5, we would like to build some intuition as to what is happening in these two key variables. The trajectory in figure 5.10 starts

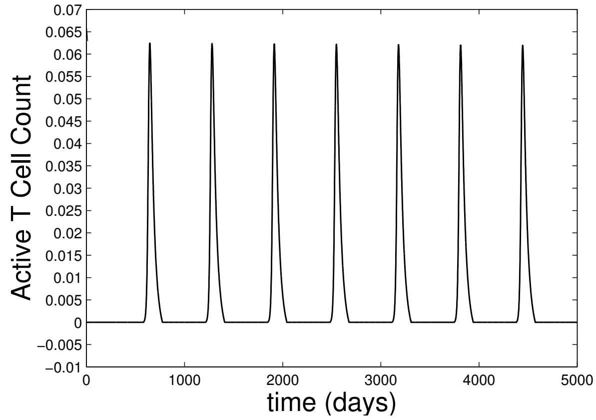

Figure 5.9: One can clearly see that the intense spikes in the active T cell population are causing the rapid and extreme oscillations in the stem cell counts. Presumably, the coefficient $\kappa_{ta} = 10$ is simply too large to reach an equilibrium with these parameter values (same as listed in table 5.1).

out near the origin, with a tiny initial abnormal cell population and no immune response. It then travels along the abnormal axis until, at a large abnormal cell value, the immune response suddenly and forcefully generates active T cells which kill the abnormal cell. This corresponds to the rapid swing in the trajectory from the lower right of the figure, to the upper left. Then, as the active T cell population subsides, the trajectory drifts back down toward the origin and the loop is repeated.

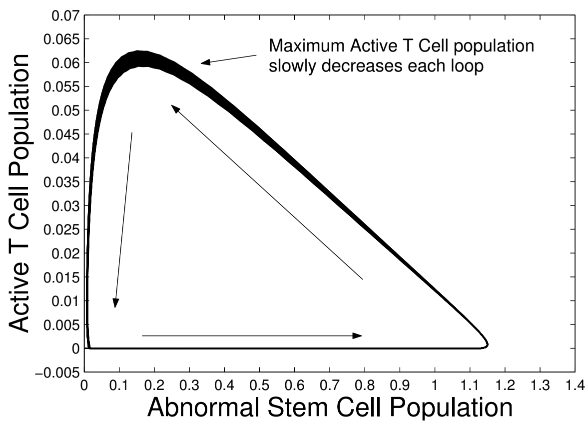

Figure 5.10: This trajectory starts near the origin and then loops around rapidly as the immune system's strong response eliminates the abnormal population. Then, as the T cells deactivate, the loop returns to the origin and continues this periodic behavior. ($\kappa_{ta} = 10$ and other parameters as listed in table 5.1)

Though the loops do not exactly overlap, their trajectory is extremely close. The slow change drift in the loops may result from the fact that our initial resting population, R, has been set very large to simulate a quasi-equilibrium. Though R does not change very quickly, it does decrease slowly which, in turn, leads to a slow downward drift in the T population. Another possibility is that the system is heading toward a stable equilibrium. If this is the case, though, it is moving so slowly that we cannot run the simulation long enough to verify this. A final possibility is that this is a homoclinic orbit.[3]

5.2.3 Immune Response Too Weak

Next, we considered the identical system, only with smaller values for κ_{ta}. We varied this parameter value from 0.01 to 0.10 and got very similar results. If one does not change the other parameters, these κ_{ta} values prove too small and the immune system has a very limited response. It appears to fight the abnormal cell population very slightly and rest in some near equilibrium position. Due to the aforementioned downward drift of R in the the model, the active T cell count then slowly drifts downward and the abnormal count rises again. One notices, though, that the amount of T cells is truly tiny ($\sim O(10^{-3})$). When this is multiplied by a small κ_{ta} value, it leaves the system in a very similar state as when the model is run without any immune intervention. Figures 5.11 and 5.12 show the progression of the stem cell populations and the active T cell populations over time, respectively. Clearly, this system behaves very similar to the system with no immune response at all.

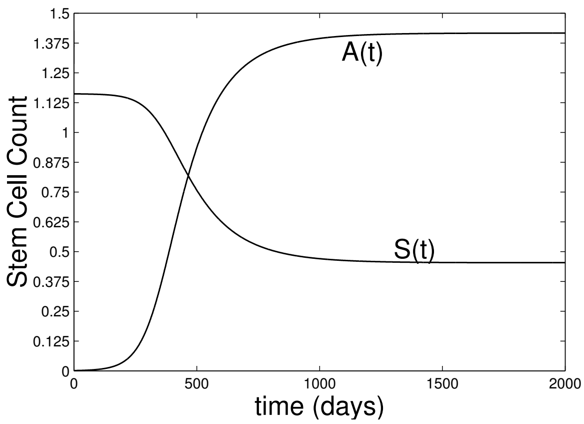

Figure 5.11: Clearly, with such a small immune response coefficient, $\kappa_{ta} = 0.01$ (other parameters as listed in table 5.1), the immune system does not really affect the populations and their trajectories strongly resemble those without any immune response.

[3]Homoclinic orbits are orbits through phase space which evolve to an unstable equilibrium over infinite time.

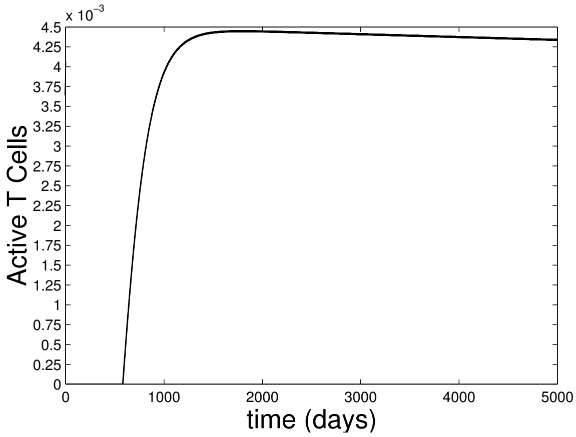

Figure 5.12: The Active T Cell Population does indeed find a quasi-equilibrium state, but its small size multiplied by a small response coefficient, $\kappa_{ta} = 0.01$ (other parameters as listed in table 5.1), renders its effects very weak.

5.2.4 Slowing Abnormal Cells by Reducing Growth Advantage

At this point, we know that we are more interested in the cases with the immune parameter closer to one, but our problem still seems to be that the immune response is not responding on a fast enough scale relative to the abnormal cells. Our first attempt to make the immune response quick involved adjusting the time scales. Clearly, this did not work sufficiently. Another way to make the immune response relatively fast is to slow down the abnormal stem cells by reducing their growth advantage. Previously set at 2, we reduce the compression or "niche" advantage to 1.05 (again, $g = 1$ corresponds to no advantage). In order to keep the parameters such that the abnormal cells do not quickly die out, we double the abnormal time scale from previous trials such that it is the same as that of the normal cells (hence, $\rho_a = 1$). We started by choosing $\kappa_{ta} = 1$ and we found that the system converged to an equilibrium without unrealistically violent oscillations. Figures 5.13 and 5.14 show the stem cells and active T cells converging over time, with some oscillations, to an equilibrium position.

Repeating the simulation with varying sizes for κ_{ta}, one finds, similarly, that the system oscillates slightly toward a stable equilibrium value. For $\kappa_{ta} \in (0.04, 3)$, we run the simulation and plot the trajectories in A,T space. We see that the equilibrium points are stable spiral nodes and that they seem to be following the curve exactly as we had hoped. Figure 5.15 shows these equilibrium values in A,T space and one notices that they start with a large value for κ_{ta} and move upward along a curve as

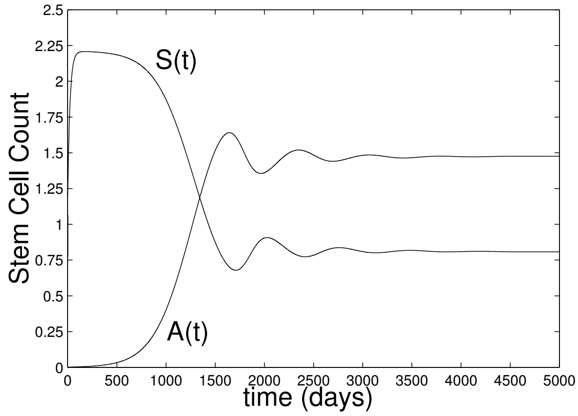

Figure 5.13: When the Abnormal Cells are slowed down by reducing their growth advantage to $g = 1.05$, we do indeed see an equilibrium emerge between all the stem cells and the immune response. The immune response does noticeably effect the stem cell populations, but they find an equilibrium value without wild oscillation. This plot shows the stem cell populations converging to that equilibrium over time. ($\kappa_{ta} = 1$, $\rho_a = 1$, $q_a = 0.125$, all other parameters are the same as in table 5.1)

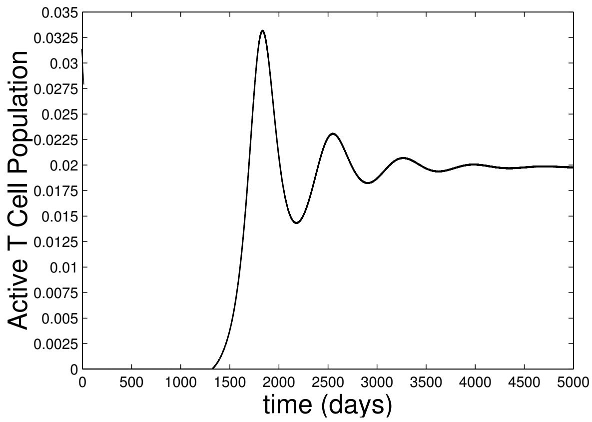

Figure 5.14: When the Abnormal Cells are slowed down by reducing their growth advantage to $g = 1.05$, the active T cell population is able to react in a less extreme manner. Rather than remaining extremely small, or periodically pulsing, the cells activate slowly and find a steady state. This plot shows the active T cell population converging to that steady state value over time. ($\kappa_{ta} = 1$, $\rho_a = 1$, $q_a = 0.125$, all other parameters are the same as in table 5.1)

we reduce κ_{ta}. The plot in figure 5.15 connects the equilibrium points for varying κ_{ta} and very much resembles the sketch in figure 5.5 which resulted from our earlier analysis. The diamonds in figure 5.15 have been added manually to emphasize the locations of the various steady states. These diamonds have then been interpolated to make the resemblance to figure 5.5 clear.

We note that when we set the κ_{ta} value at 0.01 or smaller, the system did not

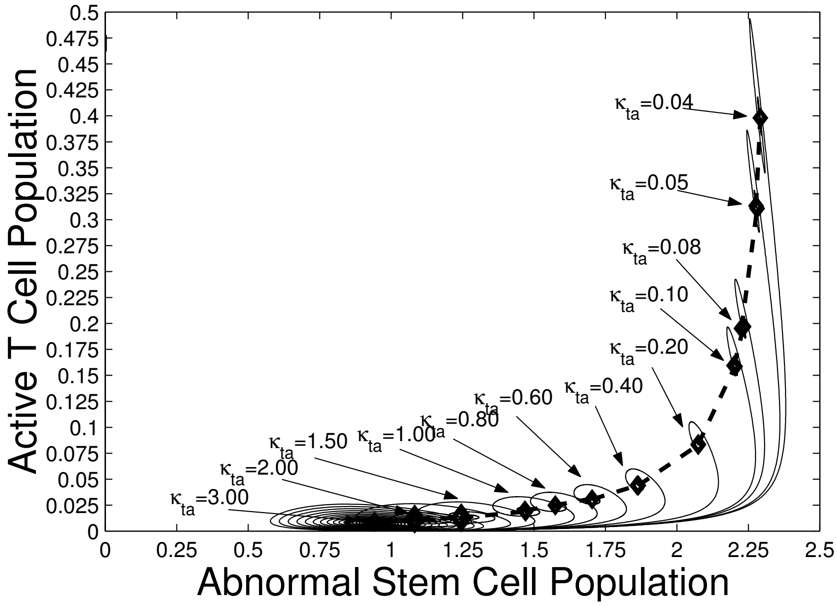

Figure 5.15: This plot shows the trajectory of many different systems whose parameters are all the same ($g = 1.05$, $q_a = 0.125$, others listed in table 5.1) except for κ_{ta}. We see the systems all spiral to stable equilibrium positions whose locations have been emphasized with the diamonds. As we decrease the immune response coefficient, κ_{ta}, the equilibrium position moves along a curve as predicted in the sketch in figure 5.5.

spiral to an equilibrium position. Rather, the active T cell count would rapidly peak to levels of about 0.14 (which had virtually no effect on the abnormal population) and then quickly return to zero.

5.2.5 Slowly Varying Immune Response

Our hypothesis was that it seemed plausible that if κ_{ta} was the slowly moving variable, the system might be in a quasi-equilibrium state, moving very slowly up the curve as κ_{ta} decreases, as shown in figure 5.15. There are a number of biological explanations why this coefficient might very slowly decrease. For instance, in Martin Nowak's models of HIV infection [30], the constant mutation of the virus causes the immune response to divide its resources among increasing amounts of different pseudo-species. In his antigenic diversity threshold model, this slow downward drift in the efficacy of the immune response leads to the transition from HIV to AIDS. Though the abnormal stem cells do not mutate in the same manner as the HIV virus does, it seems reasonable that further mutations could occur which might dilute the immune response. Another possibility would simply be that when T cells are able to focus on a small number of abnormal cells, they may be more efficient than when they are constantly fighting extremely large amounts of abnormal cells. Furthermore, if the initial equilibrium value is very close to the "nose" from figures 5.5 and 5.15, then this drift could be very small and still propel the system off of the equilibrium manifold.

To test this idea, we slightly alter the program[4] and instead of keeping κ_{ta} constant, we allow it to slowly decrease with time. Indeed, the abnormal stem cell population and the active T cell population oscillate toward an equilibrium which very slowly drifts. This drift is such that the equilibrium position involves more abnormal stem cells as well as more active T cells. At some critical point, the equilibrium manifold folds over and the new equilibrium position involves less abnormal cells than the previous position. This equilibrium is unstable and the system falls off this manifold resulting in a sharp increase in abnormal stem cell count. Depending on this drift and the parameter values, this sharp increase may include a larger number of active T cells, or it may mean the elimination of the active T cell population.

Figure 5.16 shows the phase portrait of a system with the same parameters as the above simulations, except that κ_{ta} begins with the high value of 4 and decreases at a rate of 0.004 per day. One can see that the system spirals in toward an equilibrium that continues to rise up the curve. Ultimately, the system falls off of that equilibrium curve with both the abnormal cell population and the active T cell population increasing.

Figure 5.17 shows the corresponding trajectory of the abnormal stem cells with time. The plot follows the trajectory of periodic CML fairly accurately. There is a sharp rise in the stem cell count lasting over three years, followed by a six year period of oscillations centered around a quasi-constant value, followed suddenly by a sharp increase in the cell count.

Finally, it is worth noting that the oscillations of the abnormal count are perfectly out of phase with the oscillations of the normal count. Though the abnormal population is larger than the normal population, this produces a smoothing effect. It is unclear how accurately cell counts in cases of CML distinguish between counts of normal cells and abnormal cells. If this distinction is not easily made, the system might not appear to be oscillating as much as it is. Further, we have more or less arbitrarily chosen this specific starting value of κ_{ta} as well as the drift rate. Choosing starting values closer to the "nose" of the equilibrium manifold results in systems with similar dynamics, but with significantly less oscillations. Choosing a slower drift leads to a longer chronic period, and the jump to the acute phase is less drastic. Many of the

[4]See Appendix B for code.

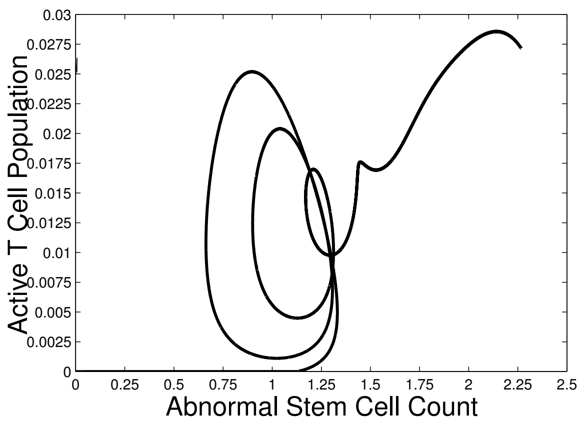

Figure 5.16: With $g = 1.05$, $q_a = 0.125$, the other parameters as in table 5.1, and $\kappa_{ta} = 4.0$, the system spirals in toward an equilibrium with a low active T cell count and a low abnormal cell count. As κ_{ta} slowly decreases (at a rate of 0.004 per day) the equilibrium moves up the vertical nullcline toward the "nose". The spirals in the phase portrait represent oscillations in the stem cell population. The system oscillates toward a slowly drifting equilibrium until κ_{ta} is sufficiently small to push that equilibrium past the bend in the equilibrium manifold. The system is sent off of the manifold and the abnormal population rapidly increases.

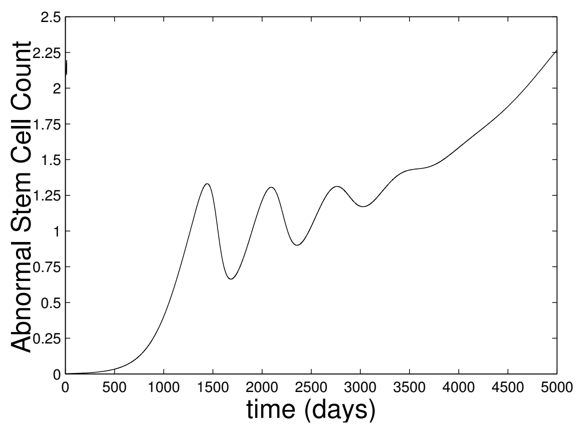

Figure 5.17: With $g = 1.05$, $q_a = 0.125$, the other parameters as in table 5.1, and $\kappa_{ta} = 4.0$, the abnormal cell population follows the progression of periodic CML or CML with oscillations during the chronic phase.

different progressions of CML can be simulated with some combination of these two parameters.

5.2.6 Slowly Increasing Resting T Cell Population

In a similar manner as in the previous subsection, we now add a drift term to the resting T cell population. First, we change the parameters such that the initial resting cell population is at 100, rather than 10,000. Further, to keep the impact of the resting T cells at a comparable level, we increase κ_{rc} from 0.001 to 0.1. We choose $\kappa_{ta} = 0.04$ as this value should put the equilibrium close to the bend in the nullcline. We then run the model with a drift of 0.5 per day in the resting T cell population. Our prediction was that this would cause the vertical nullcline to shift left and this, in turn, would correspond to a shift up and right in the equilibrium position, ultimately leading it over the bend. Though we do find that the nullcline shifts to the left, we find that the equilibrium position shifts left as well until, ultimately, it does fall off the equilibrium and exhibit oscillatory instability. This is shown in the phase portrait in figure 5.18. One plausible explanation for the fact that the equilibrium value shifts left in this phase portrait has to do with the fact that the nullcline's intercept with the A axis is fixed. Hence, the leftward shift of the nullcline is not uniform and may cause the nullcline's curvature to decrease. Though this would still ultimately cause the system to "fall off" the curve, it could also explain the leftward drift of the equilibrium position.

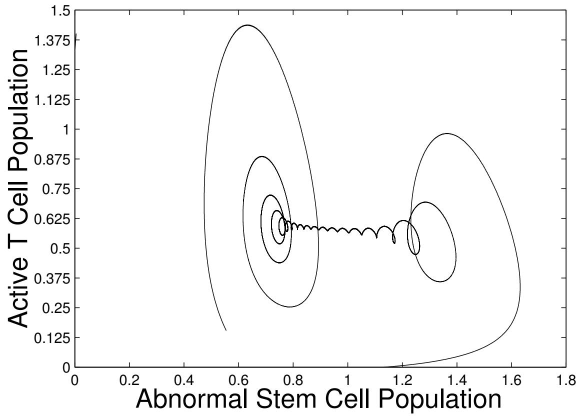

Figure 5.18: With $\kappa_{ta} = 0.4$, $g = 1.05$, $q_a = 1.25$, and all the other parameters as in table 5.1, an increase in the resting T cell population, R, at a rate of 0.5 per day, will slowly lead the system to fall off of the equilibrium manifold and become unstable.

The slow drift of the resting T cell population results in a quasi-steady state for quite a long time and then rapidly becomes unstable. The quasi-steady portion of this model lasts significantly longer than the chronic phase of CML lasts. One can alter the duration of the quasi-steady period in the trajectory, though, by choosing κ_{ta} such that the system is closer to the bend in the equilibrium manifold. Also, the quasi-equilibrium in the trajectory clearly involves a downward drift. Though this downward tendency is inconsistent with CML, the most important characteristic of the model is that it gives a plausible explanation as to how there could be a long period of quasi-stability which suddenly gives rise to violent instability. From this perspective, the trajectory of the abnormal stem cells over time, shown in figure 5.19, resembles the progression of CML quite well.

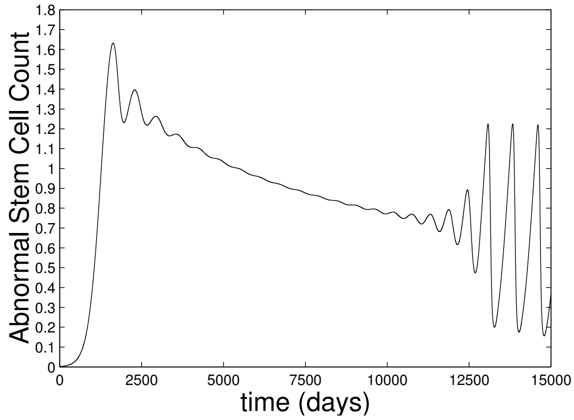

Figure 5.19: With $\kappa_{ta} = 0.4$, $g = 1.05$, $q_a = 1.25$, and all the other parameters as in table 5.1, an increase in the resting T cell population, R, at a rate of 0.5 per day, allows the abnormal cell population to travel along a quasi equilibrium at a very slow rate. Ultimately, the system falls off of this equilibrium and becomes oscillatory unstable.

Chapter 6

Results and Conclusions

6.1 Focus and Direction

The principle focus in this paper was the exploration of mechanisms by which the slow evolution of a quasi-steady state (as in CML) or a cycle of oscillations (as in pCML) could, after several years, cause a system to become unstable. The presence in CML of both a slowly moving chronic phase and a rapidly growing or oscillating acute phase suggests that some of the biological dynamics of the disease progress on a slow time scale while others have a very fast time scale. Our search for these two components of the system directed our study and provided a basic framework for our understanding of Chronic Myelogenous Leukemia.

6.2 Trajectory of Research

Once we grasped the basic biology of the system, we built an extremely simple model in order to gain a basic intuition about the progression of the disease. Though our logistic growth model was incredibly simple relative to the models used at the end of this paper, it accurately addressed the importance of the "niche" or compression advantage (g). Further, the logistic model gave us insight as to the conditions necessary for the existence and stability of a third positive steady state. Our understanding of these two concepts proved very important when analyzing the more complex models.

Next, we adapted our model to the G_0 model for the stem cell cycle. One characteristic of this model which immediately prompted our attention was the delay factor involved in the reproductive cycle. Delays commonly cause oscillations and instabilities in biological systems and given the nature of CML, it seemed particularly plausible that the delay was the key factor in the model. We performed linear stability analysis to assess this possibility and did find that the delay could produce oscillatory instability. The size of the delay required to cause these oscillations, though, severely exceeded an amount of time which seems biologically plausible and hence, we decided to explore whether the immune response could cause the slow drift leading to an instability.

In Chapter 5, we added the immune system to our model, primarily in the form of the dendritic stimulation of active T cells. We focused on this facet of the far more complex dynamics of the actual immune system because we recognized that abnormal cells would slowly give rise to abnormal dendrites. These abnormal dendrites do not recognize the abnormal stem cells as targets for the immune system and, essentially, shut down the immune response. Initially, we considered the possibility that the percentage of dendrites which could recognize the abnormal stem cells was our key slowly drifting variable. This transition, though, proved quicker than we expected and this caused us to realize that the immune response as a whole would be relatively fast compared with the growth of the abnormal cells.

6.3 Results

With our assumption that the immune response was fast, we felt we could interpret the eight-dimensional model in the reduced phase portrait of A,T space. Once we discovered that the vertical nullcline in this phase portrait was nonmonotonic with A, we immediately began to consider how slowly drifting parameters or variables might cause the system to "fall off" this equilibrium curve. Our first concept was that a slow downward drift of the mass action constant for the immune response, κ_{ta}, could result in a long quasi-equilibrium suddenly becoming unstable. Indeed, this idea worked and the fundamental characteristics of the resulting trajectory closely resembled those of periodic Chronic Myelogenous Leukemia.

After seeing the effect of a slowly drifting immune response coefficient, we realized that a slow upward drift in the resting T cell population could cause a similar progression. Though this drift resulted in a slightly decreasing quasi-steady state in the abnormal stem cell population and evolved over an exceedingly long time scale, this can, to a large extent, be attributed to the initial population values and the rate of the drift (both were chosen more or less arbitrarily). The importance of this final simulation lies in the validation of our argument that this slow drift in the resting T cell population could indeed result in a slow progression to an unstable trajectory.

6.4 Additions to the Model

A number of additions might be made to further versions of our model. One might indeed want to create second and third mutations with different growth advantages. Perhaps the system is significantly different with three competing populations rather than two. One might also consider adding the delay factor into the model with the immune response. Though the program used to solve the delay differential equations was successful in the two dimensional model, it was fantastically slow in solving the eight dimensional model. It would be interesting to see the effect of these delays in our final version of the model. The most important improvement that could be made, though, would be to make the model age-dependent. One fundamental flaw with this paper's approach is that it is difficult to compare the results to biological data. The ratio of abnormal to normal cells varies from 1 to 100 depending on which compartment, or level of development and differentiation, one chooses to measure. Our model can only aim for a ratio somewhere within this broad range.

6.5 Comparison to Models of HIV/AIDS

The fact that CML involves a steady state which lasts quite a long time and suddenly progresses to an acute phase conjures obvious comparison to the transition from HIV to AIDS. Indeed, many mathematical models of HIV can be characterized by a similar search for a slowly drifting variable. Martin Nowak's research has involved the slow dilution of the immune response as the HIV population develops a greater diversity by means of slight mutations [30]. A recent article by Alan Perelson and Patrick Nelson details their work over the last several years on models of the HIV infection [31]. They explain that many important biological processes involved in the infection occur on a number of different time scales, "from hours and days to weeks and months." As was the case for several of the initial trials in this paper, they explain that misinterpretation of the time scales of these processes can render completely incorrect concepts of what happens in the system.

6.6 Complexity of the Model

Alan Perelson's article also explains that their model does not address many of the physical, spatial realities of the immune response and drug treatment. This is similar to the limitation in our model that results from our assumption of the equal distribution of stem cells and agents of the immune response throughout the blood. In comparing our paper on CML to Perelson's paper on HIV and other papers in mathematical biology, one notices that they all seem to start with the most basic, simplified model and slowly add on layers of complexity. When working with a complex system, much of the modelling process involves choosing which elements are important and which may be ignored. In the 1950's, the cybernetician Ross Ashby coined the concept of "requisite complexity" of models [23]. In creating our mathematical model of CML, among the most difficult tasks was choosing the level of biological complexity to include in the model. Perhaps as we create more mathematical models which successfully describe biological systems, we will understand more fully the "requisite complexity" for useful models of diseases such as CML.

Appendix A

transcalc.m

The following program was writen in MATLAB and used to solve the transcendental equation 3.38 and generate a plot for equation 3.37.

```
% Defining Initial Variables

v= .001:.001:5;
w= 1*ones(size(v));
mu=1*ones(size(v));

% Iteration

for i = 1:length(v),
    tol = 10;
    wn0=3*pi/4;
    while (abs(tol)>=.0001),
       wn1=atan(-wn0/v(i))+pi;
       tol = wn1-wn0;
       wn0=wn1;
    end
    w(i)=wn1;
end
mu=v.*sec(w);

% Plotting

H = subplot(2,1,1);
plot(v,w,'r-')
xlabel('v')
ylabel('w')
subplot(2,1,2);
plot(v,mu,'k-')
xlabel('v')
ylabel('mu')
hold on;
plot(v,v,'g-')
plot(v,-v,'g-')
```

Appendix B

Programs for use with dde23.m

The following programs were written in MATLAB and use the programs dde23.m, ddeget.m, ddeset.m, and ddeval.m [34], to solve delay differential equations and generate plots.

B.1 singpop.m

```
%Define Function

function v = singpopf(t,y,Z)
v = 1.8*Z/(1+Z^2)-y/(1+y^2)-.125*y;

% Execute Program dde23('function',delay,initial value,[time span])

sol = dde23('singpopf',.566,0.001,[0,200]);
t=linspace(.566,200,1000);
y=ddeval(sol,t);
plot(t*5,y);
title('Trajectory of Delay Differential Equation with Delay of 0.566')
xlabel('time (days)');
ylabel('y(t)');
```

B.2 twopop.m

```
%Define Function

function v = twopopf(t,y,Z,a,g,qs,b,rho,qa)
ylag = Z(:,1);
v = zeros(2,1);

v(1) = 2*(1-a)*ylag(1)/(1+(g*ylag(1)+ylag(2))^2)-y(1)/(1+(g*y(1)+y(2))^2)-qs*y(1);
v(2) = 2*(1-b)*rho*ylag(2)/(1+(ylag(1)+ylag(2))^2)-rho*y(2)/(1+(y(1)+y(2))^2)-qa*y(2);

% Execute Program dde23('function',delay,initial value,[time span])
```

```
a=.1;
g=2;
qs=.125;
b=.1;
rho=1;
qa=.125/g;

sol = dde23('twopopf',.566,[2.32;0.001],[0,200],[],a,g,qs,b,rho,qa);

figure
plot(sol.x*5,sol.y);
xlabel('time t');
ylabel('y(t)');
```

B.3 delays.m

```
%Define Function

function v = delaysf(t,y,Z)
ylag1 = Z(:,1);
ylag2 = Z(:,2);
v = zeros(2,1);
a = 0.1;
b = 0.05;
qs = 0.125;
g = 2;
qa = qs/g;
rho = 0.8;

v(1) = 2*(1-a)*ylag1(1)/(1+(g*ylag1(1)+ylag1(2))^2)-y(1)/(1+(g*y(1)+y(2))^2)-qs*y(1);
v(2) = 2*(1-b)*rho*ylag2(2)/(1+(ylag2(1)+ylag2(2))^2)-rho*y(2)/(1+(y(1)+y(2))^2)-qa*y(2);

% Execute Program dde23('function',delay,initial value,[time span])

sol = dde23('delaysf',[.566,11],[2.4;0.001],[0,2000]);

figure
plot(sol.x*5,sol.y);
hold on; plot(sol.x*5,(sol.y(1,:)+sol.y(2,:)),'r');
xlabel('time (days)');
ylabel('y(t)');
```

B.4 immune1.m

```
%Define Function

function v = immune1f(t,y,z)
ylag1 = Z(:,1);
ylag2 = Z(:,2);
ylag3 = Z(:,3);
ylag4 = Z(:,4);
```

```
v = zeros(8,1);
g = 2;
a = 0.1;
b = 0.05;
qs = 0.125;
qa = 0.1;
qd = 0.1;
qx = 5;
qad = 0.01;
rhoa = 0.5;
rhod = 0.1;
rhox = 1;
kappata = .01;
kappada = 0.1;
kappaxt = 0.2;
kapparc = 0.001;
kappact = 0.15;
C0 = 0.1;

v(1) = 2*(1-a)*ylag1(1)/(1+(g*ylag1(1)+ylag1(2))^2)-y(1)/(1+(g*y(1)+y(2))^2)-qs*y(1);
v(2) = 2*(1-b)*rhoa*ylag2(2)/(1+(ylag2(1)+ylag2(2))^2)-rhoa*y(2)/(1+(y(1)+y(2))^2)-qa*y(2)-
kappata*y(8)*y(2);
v(3) = rhod*ylag3(1)-qd*y(3)-kappada*y(3)*y(5);
v(4) = rhox*ylag4(2)-qx*y(4);
v(5) = qad*y(2)+kappata*y(8)*y(2)-kappada*y(3)*y(5);
v(6) = kappada*y(3)*y(5)-qd*y(6);
if (y(6)-C0) >= 0
   v(7) = kappaxt*y(4)*y(8)-kapparc*y(7)*(y(6)-C0);
else
   v(7) = kappaxt*y(4)*y(8); end
if (y(6)-C0) >= 0
   v(8) = kappact*y(6)*y(8)+kapparc*y(7)*(y(6)-C0)-kappaxt*(y(4)+y(3))*y(8);
else
   v(8) = kappact*y(6)*y(8)-kappaxt*(y(4)+y(3))*y(8); end

% Execute Program dde23('function',delay,initial value,[time span])

sol = dde23('immune1f',[.566,.566,8.4,8.4],[1.162;0.001;1.162;0;0;0;10000;0],[0,800]);

figure
plot(sol.x*5,sol.y(1:2,:)); hold on;
xlabel('time (days)');
ylabel('y(t)');
```

immune1.m was easily and quickly altered to allow for a slow drift of the κ_{ta} term. I eliminated it from the initial variable declarations and inserted it as v(9), making the model nine dimensional[1]. Next, I replaced kappata with y(9) everywhere. When I called the program, as an argument I gave it an initial value. By setting v(9) =

[1]One does have to alter the dimensions of all relevant variables, like setting v = zeros(9,1) (rather than v = zeros(8,1)), etc., to ensure consistency.

-0.0001, for instance, I could give it a very slow downward drift. The upward drift in the population of resting T cells, R, was simulated in an identical manner.

Bibliography

[1] Bruce Alberts, Dennis Bray, Julian Lewis, Martin Raff, Keith Roberts, and James D. Watson. *Molecular Biology of The Cell.* Garland Publishing, Inc., 1994.

[2] A.D. Bates, A.G. McLennan, P.C. Turner, and M.R.H. White. *Instant Notes in Molecular Biology.* Bios Scientific Publishers, 1997.

[3] Ernest Beutler, Barry S. Coller, Marshall A. Lichtman, and Thomas J. Kipps. *Williams Hematology.* McGraw Hill, 1995.

[4] John Burthem. Lecture notes taken at talk at ociam. *Oxford University*, 2000.

[5] B. D. Clarkson, A.S Fokas, and J.B. Keller. Mathematical model of granulocytopoiesis and chronic myelogenous leukaemia. *Cancer Research*, **51**:2084–2091, 1991.

[6] Bayard Clarkson and Annabel Strife. Biology of chronic myelogenous leukemia: Is discordant maturation the primary defect? *Seminars in Hematology*, **25 No. 1**:1–19, 1988.

[7] Bayard D. Clarkson, Annabel Strife, Fried Jerrold, and Subhash Gulati. Cytokinetics and cancer treatment. *Accomplishments in Oncology*, pages 131–192.

[8] Ramzi S. Cotran, Vinay Kumar, and Stanley L. Robbins. *Robbins Pathologic Basis of Disease.* W.B. Saunders Company, 1989.

[9] David C. Dale, Caroline Haurie, and Michael C. Mackey. Cyclical neutropenia and other periodic hematological disorders: A review of mechanisms and mathematical models. *Blood*, **92 No. 8**:2629–2640, 1998.

[10] David C. Dale, Caroline Haurie, and Michael C. Mackey. Occurrence of periodic oscillations in the differential blood counts of congenital, idiopathic, and cyclical neutropenic patients before and during treatment with g-csf. *Experimental Hematology*, **27**:401–409, 1999.

[11] Martin Dunitz. *An Atlas of Malignant Haemmatology: Cytology, Histology, and Cytogenesis*. London, 1996.

[12] Pascal Fortin and Michael C. Mackey. Periodic chronic myelogenous leukaemia: spectral analysis of blood cell counts and aetiological implications. *British Journal of Haematology*, **104**:336–345, 1998.

[13] A. C. Fowler. *Mathematical Models in the Applied Sciences*. Cambridge Texts in the Applied Mathematics, 1997.

[14] A. C. Fowler and G.P. Kalamangalam. The role of the central chemoreceptor in causing periodic breathing. *IMA Journal of Mathematics Applied in Medicine and Biology*, **17**:147–167, 2000.

[15] Mel F. Greaves, Edward S. Henderson, and T. Andrew Lister. *Leukemia: Sixth Edition*. Saunders, 1996.

[16] I. Gyori and G. Ladas. *Oscillation Theory of Delay Differential Equations*. Clarendon Press, 1991.

[17] G. Hall and J.M. Watt. *Modern Numerical Methods for Ordinary Differential Equations*. Clarendon Press, 1976.

[18] F. G. J. Hayhoe and D. Quaglino. *Haematological Oncology: Clinical Practice*. Churchill Livingstone, 1992.

[19] Merck Inc. *CD4 Cell Count*. Found at http://www.merck.com/, 2000.

[20] WebMd Heath Inc. *Info: White Blood Cell Counts*. Found at http://my.webmd.com/, 2000.

[21] James H. Jandl. *Blood: Pathophysiology*. Blackwell Scientific Publications, Inc., 1991.

[22] Charles A. Janeway and Paul Travers. *Immuno Biology*. Current Biology, 1996.

[23] Kevin Kelly. *Out of Control.* Perseus Books, 1994.

[24] Johann Kummermehr and Klaus-Rudiger Trott. Tumour stem cells. *Stem Cells*, **Academic Press**:363–399, 1997.

[25] Brian I. Lord. Biology of the haemopoietic stem cell. *Stem Cells*, **Academic Press**:401–419, 1997.

[26] Michael C. Mackey. Cell kinetic status of hematopoietic stem cells. *Pending*, 2000.

[27] Michael C. Mackey. Lecture notes taken at talk at ociam. *Oxford University*, 2000.

[28] Michael C. Mackey and Joanna L. Swinburne. Cyclical thrombodytopenia: Characterization by spectral analysis and a review. *Journal of Theoretical Medicine*, **2**:81–91, 2000.

[29] J.D. Murray. *Mathematical Biology.* Springer-Verlag, 1993.

[30] Martin Nowak and Robert M. May. Mathematical biology of hiv infections: Antigenic variation and diversity threshold. *Mathematical Biosciences*, **106**:1–21, 1991.

[31] Alan S. Perelson and Patrick W. Nelson. Mathematical analysis of hiv-1 dynamics in vivo. *SIAM Review*, **41 No. 1**:3–44, 1999.

[32] Lee A. Segel. *Modeling dynamic phenomena in molecular and cellular biology.* Cambridge University Press, 1984.

[33] Lawrence F. Shampine. *Numerical Solution of Ordinary Differential Equations.* Chapman & Hall, 1994.

[34] L.F. Shampine and S. Thompson. *Solving DDEs in MATLAB.* Found at http://www.runet.edu/ thompson/webddes/, 2000.

[35] Judy Tam. Delay effect in a model for virus replication. *IMA Journal of Mathematics Applied in Medicine and Biology*, **16**:29–37, 1999.

[36] J. A. Whittaker. *Leukaemia.* Blackwell Scientific Publications, 1987.